

A-POLYNOMIALS, PTOLEMY VARIETIES AND DEHN FILLING

JOSHUA A. HOWIE, DANIEL V. MATHEWS, AND JESSICA S. PURCELL

ABSTRACT. The A-polynomial encodes hyperbolic geometric information on knots and related manifolds. Historically, it has been difficult to compute, and particularly difficult to determine A-polynomials of infinite families of knots. Here, we show how to compute A-polynomials by starting with a triangulation of a manifold, similar to Champanerkar, then using symplectic properties of the Neumann-Zagier matrix encoding the gluings to change the basis of the computation. The result is a simplification of the defining equations. Our methods are a refined version of Dimofte’s symplectic reduction, and we conjecture that the result is equivalent to equations arising from the enhanced Ptolemy variety of Zickert, which would connect these different approaches to the A-polynomial.

We apply this method to families of manifolds obtained by Dehn filling, and show that the defining equations of their A-polynomials are Ptolemy equations which, up to signs, are equations between cluster variables in the cluster algebra of the cusp torus. Thus the change in A-polynomial under Dehn filling is given by an explicit twisted cluster algebra. We compute the equations for Dehn fillings of the Whitehead link.

1. INTRODUCTION

In this paper, we show that the deformation variety used by Champanerkar in [2] to compute the $\mathrm{PSL}(2, \mathbb{C})$ A-polynomial can be defined by simpler equations, each at most a degree two polynomial in the variables that are eliminated to produce the A-polynomial. Moreover, these simple equations exhibit an algebraic structure related to that of cluster algebras, and we conjecture they essentially describe the extended Ptolemy variety of Zickert [29]. These simple equations can be written explicitly for many examples.

1.1. Computing the A-polynomial: historical context. A-polynomials were first defined for knot complements in [3], and the first computations of examples used algebraic tools, for example as in [4].

Champanerkar introduced a geometric way to compute the A-polynomial [2], based on a triangulation of the knot complement. To obtain the polynomial, up to technicalities, start from a collection of equations — one gluing equation for each edge, and two equations for the cusp — and eliminate variables. The variables are tetrahedron parameters z_i , and parameters ℓ and m for the holonomy of a longitude and a meridian. Eliminating the variables z_i gives a polynomial relation between ℓ and m which (technicalities aside) is the A-polynomial. While the defining equations of Champanerkar are satisfyingly geometric, unfortunately they can have very high degree, and underlying algebraic structure is not clear from the list of equations.

Zickert introduced a new way to compute A-polynomials in his work on extended Ptolemy varieties [29], extending work of Garoufalidis–Thurston–Zickert [11] that was inspired by Fock and Goncharov [8]. This work also starts with a triangulation, but in the case of interest assigns six variables per tetrahedron, and relates these by what are called Ptolemy relations and identification relations. The latter identify variables with an appropriate sign under gluing. After an appropriate transformation, the corresponding variables satisfy gluing equations; see [11, Section 12]. Zickert notes again a “fundamental duality” between Ptolemy coordinates and gluing equations in [29, Remark 1.13]. However, it is not clear why the duality arises.

In this paper, we show that Champanerkar’s formulation is equivalent to one involving Ptolemy-like relations, similar to those defining the enhanced Ptolemy variety of Zickert, but with fewer

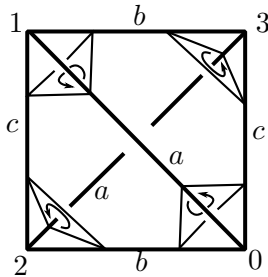


FIGURE 1. A tetrahedron with vertices labeled 0, 1, 2, 3 and opposite edges labeled a , b , c .

variables. Thus, we expect that the results of this paper provide a connection between two rather different approaches to calculating A-polyomials. Though we do not show that these two approaches are equivalent, we conjecture that this method gives a $\mathrm{PSL}(2, \mathbb{C})$ version of the enhanced Ptolemy variety. It may provide an explanation for the “fundamental duality” between shape coordinates and Ptolemy coordinates noted in [11, 29].

Our method is to apply and refine work of Dimofte [6, 7], from physics. The coefficients in the gluing and cusp equations are effectively the entries in the Neumann–Zagier matrix [22]. This matrix is known to have interesting symplectic properties: its rows form part of a standard symplectic basis for a symplectic vector space. Dimofte considered extending this collection of vectors into a standard basis for \mathbb{R}^{2n} , and then changing the basis. The basis changes from a standard basis indexed by tetrahedra, to a standard basis indexed by edges of the triangulation, a longitude and a meridian. This change of basis yields a change of variables, which can be applied to the gluing equations and equations for ℓ and m . The result is an equivalent set of equations, and these equations exhibit Ptolemy-like characteristics. Eliminating variables again yields (up to technicalities) the A-polynomial; effectively this can be considered a process of symplectic reduction.

There are a few issues with Dimofte’s calculations that have made them difficult to use in practice. First, the result appears in physics literature, which makes it somewhat difficult for mathematicians to read. More importantly, to carefully perform the change of basis, in particular to nail down the correct signs in the defining equations, a priori one needs to determine the symplectic dual vectors to the vectors arising from gluing equations. These are not only nontrivial to compute, but also highly non-unique. Only after obtaining such vectors can one invert a large symplectic matrix.

In this paper, we overcome these issues. Using work of Neumann [21], we show that we may “invert without inverting.” That is, we show that Dimofte’s symplectic reduction can be read off of ingredients already present in the Neumann–Zagier matrix, without having to compute symplectic dual vectors. As a result, we may convert Champanerkar’s (possibly complicated) equations into simpler equations that have Ptolemy-like structure.

Before stating the equations, we briefly review Neumann–Zagier matrices and necessary terminology.

1.2. Review of Neumann–Zagier matrices and the main theorem. Throughout this paper, M denotes a connected cusped orientable 3-manifold with an ideal triangulation consisting of n tetrahedra $\Delta_1, \dots, \Delta_n$, and hence with n edges E_1, \dots, E_n . Each tetrahedron has three pairs of opposite edges: we label these the a -edges, b -edges and c -edges, so that around each vertex the incident a -, b - and c edges are in anticlockwise order. We also label ideal vertices of tetrahedra 0, 1, 2, 3 so that the a -edges run between vertices 0 and 1 and between 2 and 3, b -edges run between 0 and 2 and between 1 and 3, and c -edges run between 0 and 3 and between 1 and 2. See Figure 1.

Recall that in the definition of Thurston's gluing equations, each hyperbolic ideal tetrahedron Δ_j has a complex-valued edge parameter z_j associated with its a -edges, edge parameter z'_j associated with its b -edges, and z''_j associated with its c -edges; see Section 2 for more details.

For the k -th edge of the triangulation, we obtain a gluing equation, indicating that edge parameters give a hyperbolic structure along the edge. The logarithm of such an equation gives an equation of the form

$$\sum_j (a_{k,j} \log z_j + b_{k,j} \log z'_j + c_{k,j} \log z''_j) = 2\pi i,$$

where $a_{k,j}, b_{k,j}, c_{k,j}$ indicate the number of a -edges, b -edges, and c -edges of Δ_j , respectively, that are glued to the k -th edge. Similarly, the meridian and longitude of the cusp, we have cusp equations of the form

$$\sum_j (a_j^m \log z_j + b_j^m \log z'_j + c_j^m \log z''_j) = \log m, \quad \text{and} \quad \sum_j (a_j^l \log z_j + b_j^l \log z'_j + c_j^l \log z''_j) = \log \ell.$$

Using the fact that $z_j z'_j z''_j = 1$, we may replace $\log z''_j$ in the above equations by terms in z_j, z'_j alone. The gluing equation becomes

$$\sum_j (a_{k,j} - c_{k,j}) \log z_j + (b_{k,j} - c_{k,j}) \log z'_j = \pi i (2 - \sum_j c_{k,j}).$$

The gluing and cusp equations in this form fit into a well-known matrix equation:

$$\begin{pmatrix} (a_{1,1} - c_{1,1}) & (b_{1,1} - c_{1,1}) & (a_{1,2} - c_{1,2}) & \cdots \\ (a_{2,1} - c_{2,1}) & (b_{2,1} - c_{2,1}) & (a_{2,2} - c_{2,2}) & \cdots \\ \vdots & \vdots & \vdots & \ddots \\ (a_{n,1} - c_{n,1}) & (b_{n,1} - c_{n,1}) & (a_{n,2} - c_{n,2}) & \cdots \\ (a_1^m - c_1^m) & (b_1^m - c_1^m) & (a_2^m - c_2^m) & \cdots \\ (a_1^l - c_1^l) & (b_1^l - c_1^l) & (a_2^l - c_2^l) & \cdots \end{pmatrix} \cdot \begin{pmatrix} \log z_1 \\ \log z'_1 \\ \log z_2 \\ \log z'_2 \\ \vdots \\ \log z_n \\ \log z'_n \end{pmatrix} = \begin{pmatrix} i\pi(2 - \sum_j c_{1,j}) \\ i\pi(2 - \sum_j c_{2,j}) \\ \vdots \\ i\pi(2 - \sum_j c_{n,j}) \\ \log m - i\pi \sum_j c_j^m \\ \log \ell - i\pi \sum_j c_j^l \end{pmatrix}$$

The matrix on the left of the equation above is the *Neumann–Zagier matrix*, denoted by NZ. The vector on the right gives sign terms. Ignoring the $i\pi$ factors and $\log m$ and $\log \ell$ terms in this vector, we define a vector C by $C = ((2 - \sum_j c_{1,j}), \dots, (2 - \sum_j c_{n,j}), -\sum_j c_j^m, -\sum_j c_j^l)$.

Neumann and Zagier showed that if M has one cusp, then any one of the rows of NZ corresponding to gluing equations can be written as a linear combination of the others, but after removing such a row, the rows can be made linearly independent. Denote the matrix given by removing such a row of NZ by NZ^b , and similarly denote the vector obtained from C by removing the corresponding row by C^b . We will refer to NZ^b as the *reduced Neumann–Zagier matrix*. The vector C^b is called the sign vector.

Note that the last two rows of the reduced Neumann–Zagier matrix NZ^b correspond to cusp equations associated to the meridian and longitude. For ease of notation, we will denote the entries in the row associated to the meridian and longitude, respectively, by

$$(\mu_1 \ \mu'_1 \ \mu_2 \ \mu'_2 \ \dots) \quad \text{and} \quad (\lambda_1 \ \lambda'_1 \ \lambda_2 \ \lambda'_2 \ \dots).$$

We will show that, after possibly relabelling the tetrahedra of a triangulation, we may assume one of the first $(n - 1)$ entries of C^b is nonzero. We call a triangulation with such a labelling *good*.

Theorem 1.1. *Let M be a one-cusped manifold with a good hyperbolic triangulation \mathcal{T} , with associated reduced Neumann–Zagier matrix NZ^b and sign vector C^b as above. Also as above, denote the entries of the last two rows of NZ^b by μ_j, μ'_j in the row corresponding to the meridian, and λ_j, λ'_j for the row corresponding to the longitude. Let $B = (B_1, B'_1, B_2, B'_2, \dots)$ be an integer vector such that $\text{NZ}^b \cdot B = C^b$, which exists due to work of Neumann [21].*

Define formal variables $\gamma_1, \dots, \gamma_n$, one associated with each edge of \mathcal{T} . For a tetrahedron Δ_j of \mathcal{T} , and $\alpha\beta \in \{01, 02, 03, 12, 13, 23\}$, define $\gamma_{j(\alpha\beta)}$ to be the variable γ_k such that the edge of Δ_j between vertices α and β is glued to the edge of \mathcal{T} associated with γ_k .

For each tetrahedron Δ_j of \mathcal{T} , define the Ptolemy equation of Δ_j by

$$(-1)^{B'_j} \ell^{-\mu_j/2} m^{\lambda_j/2} \gamma_{j(01)} \gamma_{j(23)} + (-1)^{B_j} \ell^{-\mu'_j/2} m^{\lambda'_j/2} \gamma_{j(02)} \gamma_{j(13)} - \gamma_{j(03)} \gamma_{j(12)} = 0.$$

When we solve the system of Ptolemy equations of \mathcal{T} in terms of m and ℓ , setting $\gamma_n = 1$ and eliminating the variables $\gamma_1, \dots, \gamma_{n-1}$, we obtain a factor of the $\mathrm{PSL}(2, \mathbb{C})$ A-polynomial, which is the same polynomial obtained by Champanerkar.

The precise version of this theorem is contained in Theorem 2.64 below. A precise version of Champanerkar's polynomial from [2] can be found in Theorem 2.15 below.

Remark 1.2. Observe that finding the A-polynomial using the gluing equations, following Champanerkar [2], gives the same number of equations as in Theorem 1.1, but in the variables z_j, z'_j, m, ℓ . However, in the gluing equations, the degrees of the variables z_j, z'_j , which must be eliminated, can be very high. By contrast, the Ptolemy equations above are always quadratic in the variables γ_j . Moreover, their form indicates intriguing algebraic structure that is not readily apparent from the gluing equations.

We find the simplicity and the algebraic structure of the equations of Theorem 1.1 to be a major feature of this paper. The defining equations of the A-polynomial are quite simple! However, we note that the *proof* of the theorem is not simple, especially if all the details are considered — and we consider details. In the course of proving the theorem, the reader will encounter hyperbolic geometry and triangulations, symplectic linear algebra, and related algebraic tools. We have attempted to make the calculations easy to read, and easy to reproduce, which has increased their length. However, we do believe that the simple payoff justifies the complicated proof.

We also note that using these equations requires finding the vector B of Theorem 1.1. This is a problem in linear Diophantine equations. Because B is guaranteed to exist, it can be found by computing the Smith normal form of the matrix NZ (see, for example, Chapter II.21(c) of [23]). In practice, we were able to find B for examples with significantly less work. In Section 3, we show that if N is a 2-cusped hyperbolic 3-manifold, then the values of B for all Dehn fillings of N along one cusp can be determined immediately from values for the unfilled manifold N . We apply this to Dehn fillings of the Whitehead link in Section 4.

Remark 1.3. The γ variables in Theorem 1.1 are precisely Dimofte's γ variables of [6], and these Ptolemy equations are essentially equivalent to those of that paper.

The word “equivalent” here conceals a projective subtlety. The gluing and cusp equations are a set of $n + 2$ equations in n tetrahedron parameters and ℓ, m , but only $n + 1$ of them are independent. The Ptolemy equations are however a set of n independent equations in n edge variables and ℓ, m . However, they are homogeneous, and so $\gamma_1, \dots, \gamma_n$ can be regarded as varying on \mathbb{CP}^{n-1} ; alternatively, one can divide through by an appropriate power of one γ_i to obtain equations in the $n - 1$ variables $\frac{\gamma_1}{\gamma_i}, \dots, \frac{\gamma_{i-1}}{\gamma_i}, \frac{\gamma_{i+1}}{\gamma_i}, \dots, \frac{\gamma_n}{\gamma_i}$, which can be eliminated. Effectively, one can simply set one of the variables γ_i to 1.

A further subtlety arises because our Ptolemy equations are *not* polynomials in m and ℓ ; they are rather polynomials in $m^{1/2}$ and $\ell^{1/2}$. If we set $M = m^{1/2}$ and $L = \ell^{1/2}$ then we obtain *polynomial* Ptolemy equations. Moreover, the variables L and M so defined are essentially those appearing in the $\mathrm{SL}(2, \mathbb{C})$ A-polynomial: a matrix in $\mathrm{SL}(2, \mathbb{C})$ with eigenvalues L, L^{-1} yields an element of $\mathrm{PSL}(2, \mathbb{C})$ corresponding to a hyperbolic isometry with holonomy $L^2 = \ell$. Indeed, the Ptolemy varieties of [29] are calculated from $\mathrm{SL}(2, \mathbb{C})$ representations, rather than $\mathrm{PSL}(2, \mathbb{C})$. We obtain the following.

Corollary 1.4. *After setting $M = m^{1/2}$ and $L = \ell^{1/2}$, eliminating the γ variables from the polynomial Ptolemy equations of a one-cusped hyperbolic triangulation yields a polynomial in M and L which contains, as a factor, the factor of the $\mathrm{SL}(2, \mathbb{C})$ A-polynomial describing hyperbolic structures.*

The precise version of this corollary is Corollary 2.65.

1.3. Ptolemy equations in Dehn filling. Our main application of Theorem 1.1 is to consider the defining equations of A-polynomials under Dehn filling.

Consider a two-component link in S^3 with component knots K_0, K_1 . Consider Dehn filling K_0 along some slope p/q ; K_1 then becomes a knot in a 3-manifold. Heuristically, as p/q becomes a more complicated fraction, a more complicated triangulation is required to triangulate the Dehn filled manifold.

A Dehn filling can be triangulated using *layered solid tori*, originally defined by Jaco and Rubinstein [17]; see also Guéritaud–Schleimer [14]. Building a layered solid torus yields a sequence of triangulations of a once-punctured torus. Moreover, the combinatorics of the 3-dimensional triangulation in the layered solid torus correspond closely to the combinatorics of 2-dimensional triangulations of punctured tori.

Triangulations of punctured tori can be endowed with λ -lengths via work of Penner [24]. When one flips a diagonal in a triangulation, the λ -lengths are related by a Ptolemy equation. This gives the algebra formed by λ -lengths the structure of a *cluster algebra* [8, 9, 12]. Cluster algebras have been found to arise in diverse contexts across mathematics (see e.g. [10, 28]).

We show that the Ptolemy equations for the cluster algebra of the punctured torus coming from λ -lengths, and the Ptolemy equations of the tetrahedra in the layered solid torus from Theorem 1.1, are identical up to sign. We can regard the algebra generated by these Ptolemy equations as a “twisted” cluster algebra.

More precisely, we show that we can take triangulations of 3-manifolds obtained by Dehn filling the initial manifold, so that the Ptolemy equations of tetrahedra outside the layered solid torus remain invariant, and so that the Ptolemy equations of tetrahedra inside the layered solid torus are those of a *twisted cluster algebra*. By “twisted” we simply mean that the Ptolemy equations are those arising in the usual cluster algebra of a punctured torus, but with some changes of sign which we will define precisely in due course.

Theorem 1.5. *Suppose M has two cusps $\mathfrak{c}_0, \mathfrak{c}_1$. Let $M_{p/q}$ be the manifold obtained from M by performing p/q surgery on \mathfrak{c}_0 . Then for an appropriate choice of triangulation and other data for $M_{p/q}$, the Ptolemy relations for the tetrahedra in the Dehn filling solid torus are those which appear in a twisted cluster algebra. They take the form*

$$\pm\gamma_x\gamma_y \pm \gamma_a^2 - \gamma_b^2 = 0,$$

where a, b, x, y are slopes on the torus boundary and x, y are crossing diagonals.

A precise version of this theorem is Theorem 3.18.

The above applies to any two-cusped connected orientable manifold. If the Dehn surgeries yield knot complements in S^3 (or more generally in a homology 3-sphere), then we can relate their A-polynomials.

Theorem 1.5 in particular implies that if we take a *sequence* of Dehn filling slopes $\{p_i/q_i\}$, corresponding to a walk in the Farey graph, then the A-polynomials of the knots $K_i = K_{p_i/q_i}$, are closely related. Then the Ptolemy equations defining $A_{K_{i+1}}$ are, roughly speaking, obtained from those for A_{K_i} by adding a single extra Ptolemy relation.

1.4. Example: Twist knots. We put this idea in to practice by considering some families of knots as examples. To illustrate briefly the *simplicity* of the resulting equations, we consider the twist knots, which are Dehn fillings of the Whitehead link. We discuss the Whitehead link and its Dehn fillings in more detail in Section 4. These knots include the twist knots, whose A-polynomials

are known to satisfy various algebraic relations [16, 19, 20]. For these knots, we obtain Ptolemy equations as follows.

We will label γ variables corresponding to edges in a layered solid torus by *slopes* in $\mathbb{Q} \cup \{\infty\}$. This notation, which we will see arises from the Farey graph, is a simplification of that in the generic equation above. Three of the Ptolemy equations agree for all twist knots, and indeed all Dehn fillings of the Whitehead link; these arise from tetrahedra outside the Dehn filling solid torus. The equations are

$$(1.6) \quad 0 = -LM^{-1}\gamma_{0(23)}\gamma_{2/1} - LM^{-2}\gamma_{3/1}\gamma_{1/0} - \gamma_{1/0}^2$$

$$(1.7) \quad 0 = -M\gamma_{3/1}\gamma_{1/0} - LM^{-1}\gamma_{1/0}^2 - \gamma_{0(23)}\gamma_{2/1}$$

$$(1.8) \quad 0 = \gamma_{1/0}^2 - \gamma_{1/0}\gamma_{3/1} - \gamma_{0(23)}^2$$

where $L = \ell^{1/2}$ and $M = m^{1/2}$.

With the standard longitude and meridian for the Whitehead link, given our triangulation, the $-1/1$ or LL filling is the figure-8 knot complement. It is obtained from gluing a layered solid torus with 2 tetrahedra. The Ptolemy equations of these two tetrahedra are

$$(1.9) \quad 0 = \gamma_{3/1}\gamma_{1/1} + \gamma_{2/1}^2 - \gamma_{1/0}^2$$

$$(1.10) \quad 0 = -\gamma_{2/1}\gamma_{0/1} + \gamma_{1/1}^2 - \gamma_{1/0}^2.$$

Folding up the layered solid torus to obtain the figure-8 knot complement yields a final equation $\gamma_{0/1} = \gamma_{1/0}$.

The $1/2$ or LR filling is the 5_2 knot complement, and is obtained from gluing the same layered solid torus, folded up a different way. So we take the Ptolemy equations above, but now set $\gamma_{1/1} = \gamma_{0/1}$.

The $1/3$ or LRL filling is the 7_2 knot, which has a layered solid torus with one more tetrahedron, with Ptolemy equation

$$(1.11) \quad 0 = \gamma_{1/0}\gamma_{1/2} + \gamma_{1/1}^2 - \gamma_{0/1}^2,$$

which we then fold up and identify $\gamma_{1/2} = \gamma_{0/1}$.

The $1/4$ or LRL filling is the 9_2 knot complement, which adds another tetrahedron with Ptolemy equation

$$(1.12) \quad 0 = -\gamma_{1/1}\gamma_{1/3} + \gamma_{1/2}^2 - \gamma_{0/1}^2,$$

folded up with identification $\gamma_{1/3} = \gamma_{0/1}$.

Observe that the set of Ptolemy equations at each step contains all those of the previous step, with one additional equation. The final folding then identifies two of the variables. In Section 4 we give the general form of Ptolemy equations for the knot complements in this sequence.

The equations and the identifications of variables will be fully explained in Section 4. The signs are determined by the left and right turns (Ls and Rs) in the word describing the associated path in the Farey graph, as we will see (Theorem 3.18).

After eliminating the γ variables from each set of equations, one obtains a polynomial in L, M which contains as a factor, up to a change of basis, the standard A-polynomial. By a change of basis in the variables L, M we mean a transformation of the form $(L, M) \mapsto (L^a M^b, L^c M^d)$ where

$$\begin{pmatrix} a & b \\ c & d \end{pmatrix} \in GL(2, \mathbb{Z}).$$

1.5. Structure of this paper. In Section 2, we recall the machinery we need from work of Thurston, and Neumann and Zagier [22], including gluing and cusp equations, the Neumann–Zagier matrix, and its symplectic properties. We introduce a symplectic change of basis, and show this leads to Ptolemy equations that give the A-polynomial.

In Section 3, we connect to Dehn fillings. Suppose two 3-manifolds with one cusp are obtained by Dehn filling the same parent manifold with two cusps; for example twist knots have this property,

with parent knot the Whitehead link. We show that the parent manifold has a triangulation for which the cusp to be filled meets exactly two ideal vertices, and for which generators of the homology on the cusp left unfilled do not meet these two ideal tetrahedra. It follows that the Dehn fillings can be obtained by replacing the two tetrahedra by a layered solid torus. We review the construction of layered solid tori in this section, and show how the triangulation adjusts the Neumann–Zagier matrix. Using this, we find Ptolemy equations for any layered solid torus. Thus the Ptolemy equations defining the A-polynomial in the case of Dehn filling can be read off of the outside of the layered solid torus, and then adjusted in a straightforward way inside the layered solid torus.

Section 4 works through some examples in detail: knots obtained by Dehn filling the Whitehead link. We give Ptolemy equations for all manifolds obtained by Dehn filling one cusp of these links, including many knot complements.

1.6. Acknowledgments. This work was supported by ARC grant DP160103085.

2. FROM GLUING EQUATIONS TO PTOLEMY EQUATIONS VIA SYMPLECTIC REDUCTION

In this section we discuss Dimofte’s symplectic reduction method and refine it to show how gluing and cusp equations are equivalent to Ptolemy equations, proving Theorem 1.1.

2.1. Triangulations, gluing and cusp equations. Let M be a 3-manifold that is the interior of a compact manifold \overline{M} with all boundary components tori. Let the number of boundary tori be n_c , so M has n_c cusps. For example, M may be a link complement $S^3 - L$, where L is a link of n_c components, and \overline{M} a link exterior $S^3 - N(L)$.

Suppose M has an ideal triangulation. Throughout this paper, unless stated otherwise, *triangulation* means ideal triangulation, and *tetrahedron* means ideal tetrahedron. Throughout, n denotes the number of tetrahedra in a triangulation.

Our tetrahedra will be labelled as follows.

Definition 2.1. An *oriented labelling* of an oriented tetrahedron is a labelling of its four ideal vertices with the numbers 0, 1, 2, 3 as in Figure 1, up to oriented homeomorphism preserving edges.

(Note that when tetrahedra are glued to form M , ideal vertices with different labels may be identified.)

In an oriented labelling of an oriented tetrahedron, the four faces, with respect to the boundary orientation, have vertices 012, 023, 031 and 321 in positive (anticlockwise) order.

Definition 2.2. In an ideal tetrahedron with an oriented labelling, we call the opposite pairs of edges (01, 23), (02, 13), (03, 12) respectively the *a-edges*, *b-edges* and *c-edges*.

In an oriented labelling, around each vertex (as viewed from outside the tetrahedron), the three incident edges are an *a-*, *b-*, and *c-*edge in anticlockwise order.

Note that an oriented tetrahedron has precisely 12 oriented labellings. These labellings are related by the permutations of the alternating group A_4 . Any such relabelling has the effect of cyclically permuting the *a-*, *b-* and *c-*edges. Equivalently, the *a*, *b* and *c* labels are permuted by an element of the alternating group $A_3 \cong \mathbb{Z}/3$. We will be less interested in the numbering of vertices than the labelling of edges as *a-*, *b-* and *c-*edges.

By a standard Euler characteristic argument, the number of edges in the triangulation is equal to the number n of tetrahedra, as follows: letting the numbers of edges and faces in the triangulation temporarily be E and F , $\partial\overline{M}$ is triangulated with $2E$ vertices, $3F$ edges and $4n$ triangles; as $\partial\overline{M}$ consists of tori, its Euler characteristic $2E - 3F + 4n$ is zero; as $2F = 4n$ then $E = n$.

Definition 2.3. A *labelled triangulation* of M is an oriented ideal triangulation of M , where

- (i) the tetrahedra are labelled $\Delta_1, \dots, \Delta_n$ in some order,
- (ii) the edges are labelled E_1, \dots, E_n in some order, and

(iii) each tetrahedron is given an oriented labelling.

We will often denote a labelled triangulation by \mathcal{T} . Later in the paper we will label edges and tetrahedra not by the list $\{1, 2, \dots, n\}$ but by other sets with n elements; the principle however is the same.

At times we will need to refer to the specific edges E_k to which specific edges of tetrahedra Δ_j are glued; hence the following definition.

Definition 2.4. For $j \in \{1, \dots, n\}$ and distinct $\mu, \nu \in \{0, 1, 2, 3\}$, the index of the edge to which the edge $(\mu\nu)$ of Δ_j is glued is denoted $j(\mu\nu)$.

In other words, the edge $(\mu\nu)$ of Δ_j is identified to $E_{j(\mu\nu)}$.

Suppose now that we have a labelled triangulation of M . To each tetrahedron Δ_j we associate three variables z_j, z'_j, z''_j . These variables are associated with the a -, b - and c -edges of Δ_j and satisfy the equations

$$(2.5) \quad z_j z'_j z''_j = -1$$

and

$$(2.6) \quad z_j + (z'_j)^{-1} - 1 = 0.$$

If Δ_j has a hyperbolic structure then these parameters are standard tetrahedron parameters; see [26]. Each of z_j, z'_j, z''_j gives the cross ratio of the four ideal points, in some order. The arguments of z_j, z'_j, z''_j respectively give the dihedral angles of Δ_j at the a -, b - and c -edges. Note that equations (2.5) and (2.6) imply that none of z_j, z'_j, z''_j can be equal to 0 or 1 (i.e. tetrahedra are nondegenerate).

Each edge of each tetrahedron Δ_j is identified to one of the E_k .

Definition 2.7. In a labelled triangulation of M , we denote by $a_{k,j}, b_{k,j}, c_{k,j}$ respectively the number of a -, b -, c -edges of Δ_j identified to E_k .

Lemma 2.8. For each fixed j ,

$$(2.9) \quad \sum_{k=1}^n a_{k,j} = 2, \quad \sum_{k=1}^n b_{k,j} = 2 \quad \text{and} \quad \sum_{k=1}^n c_{k,j} = 2.$$

Proof. Each tetrahedron Δ_j has two a -edges, two b -edges and two c -edges, so for fixed j the total sum over all k must be 2. \square

The nonzero terms in the first sum are $a_{j(01),j}$ and $a_{j(23),j}$. Note that $j(01)$ could equal $j(23)$; this occurs when the two a -edges of Δ_j are glued to the same edge. In that case, $a_{j(01),j}$ and $a_{j(23),j}$ are the same term, equal to 2. If the two a -edges are not glued to the same edge, then $E_{j(01)}$ and $E_{j(23)}$ are distinct, each with one a -edge of Δ_j identified to it, and $a_{j(01),j} = a_{j(23),j} = 1$. Similarly, the nonzero terms in the second sum are $b_{j(02),j}, b_{j(13),j}$ and in the third sum $c_{j(03),j}, c_{j(12),j}$.

The numbers $a_{k,j}, b_{k,j}, c_{k,j}$ can be arranged into a matrix.

Definition 2.10. The *incidence matrix* In of a labelled triangulation \mathcal{T} is the $n \times 3n$ matrix whose k th row is $(a_{k,1}, b_{k,1}, c_{k,1}, \dots, a_{k,n}, b_{k,n}, c_{k,n})$.

Thus In has rows corresponding to the edges E_1, \dots, E_n , and the columns come in triples with the j th triple corresponding to the tetrahedron Δ_j .

The *gluing equation* for edge E_k is then

$$(2.11) \quad \prod_{j=1}^n z_j^{a_{k,j}} (z'_j)^{b_{k,j}} (z''_j)^{c_{k,j}} = 1.$$

When the ideal triangulation \mathcal{T} is hyperbolic, the gluing equations express the fact that tetrahedra fit geometrically together around each edge.

Denote the n_c boundary tori of \overline{M} by $\mathbb{T}_1, \dots, \mathbb{T}_{n_c}$. A triangulation of M by tetrahedra induces a triangulation of each \mathbb{T}_k by triangles. On each \mathbb{T}_k we choose a pair of oriented curves $\mathfrak{m}_k, \mathfrak{l}_k$ forming a basis for $H_1(\mathbb{T}_k)$. By an isotopy if necessary, we may assume each curve is in general position with respect to the triangulation of \mathbb{T}_k , and without backtracking. Then each curve splits into segments, where each segment lies in a single triangle and runs from one edge to a distinct edge. Each segment of \mathfrak{m}_k or \mathfrak{l}_k can thus be regarded as running clockwise or anticlockwise around a unique corner of a triangle. We count anticlockwise motion around a vertex as positive, and clockwise motion as negative. Each vertex (resp. face) of the triangulation of \mathbb{T}_k corresponds to some edge (resp. tetrahedron) of the triangulation \mathcal{T} of M ; thus each corner of a triangle corresponds to a specific edge of a specific tetrahedron.

Definition 2.12. The *a-incidence number* (resp. *b-, c-incidence number*) of \mathfrak{m}_k (resp. \mathfrak{l}_k) with the tetrahedron Δ_j is the number of segments of \mathfrak{m}_k (resp. \mathfrak{l}_k) running anticlockwise (i.e. positively) through a corner of a triangle corresponding to an *a*-edge (resp. *b-, c*-edge) of Δ_j , minus the number of segments of \mathfrak{m}_k (resp. \mathfrak{l}_k) running clockwise (i.e. negatively) through a corner of a triangle corresponding to an *a*-edge (resp. *b*-edge, *c*-edge) of Δ_j .

- (i) Denote by $a_{k,j}^{\mathfrak{m}}, b_{k,j}^{\mathfrak{m}}, c_{k,j}^{\mathfrak{m}}$ respectively the *a-, b-, c*-incidence numbers of \mathfrak{m}_k with Δ_j .
- (ii) Denote by $a_{k,j}^{\mathfrak{l}}, b_{k,j}^{\mathfrak{l}}, c_{k,j}^{\mathfrak{l}}$ respectively the *a-, b-, c*-incidence numbers of \mathfrak{l}_k with Δ_j .

To each cusp torus \mathbb{T}_k we associate two variables m_k, ℓ_k . The *cuspidal equations* at \mathbb{T}_k are

$$(2.13) \quad m_k = \prod_{j=1}^n z_j^{a_{k,j}^{\mathfrak{m}}} (z'_j)^{b_{k,j}^{\mathfrak{m}}} (z''_j)^{c_{k,j}^{\mathfrak{m}}}$$

$$(2.14) \quad \ell_k = \prod_{j=1}^n z_j^{a_{k,j}^{\mathfrak{l}}} (z'_j)^{b_{k,j}^{\mathfrak{l}}} (z''_j)^{c_{k,j}^{\mathfrak{l}}}$$

When \mathcal{T} is a *hyperbolic triangulation*, meaning the ideal tetrahedra are all positively oriented and glue to give a smooth, complete hyperbolic structure on the underlying manifold, the cuspidal equations give m_k and ℓ_k , the holonomies of the cusp curves \mathfrak{m}_k and \mathfrak{l}_k , in terms of tetrahedron parameters.

Any hyperbolic triangulation \mathcal{T} gives tetrahedron parameters z_j, z'_j, z''_j and cusp holonomies m_k, ℓ_k satisfying the relationships (2.5)–(2.6) between the z -variables, the gluing equations (2.11) and cuspidal equations (2.13)–(2.14); moreover, the tetrahedron parameters all have positive imaginary part. However, in general there may be solutions of these equations which do not correspond to a hyperbolic triangulation, for instance those with z_j with negative imaginary part (which may still give M a hyperbolic structure), or with branching around an edge (which will not). Additionally, not every hyperbolic structure on M may give a solution to the gluing and cuspidal equations, since the triangulation \mathcal{T} may not be geometrically realisable.

2.2. The A-polynomial from gluing and cuspidal equations. Suppose now that $n_c = 1$, i.e. M has one cusp, and moreover, that M is a knot complement in a homology 3-sphere. For our examples however we will only consider knot complements in S^3 .

In this case, there is no need for the $k = 1$ subscript in notation for the lone cusp, and we may simply write

$$\begin{aligned} \mathfrak{m} &= \mathfrak{m}_1, & \mathfrak{l} &= \mathfrak{l}_1, & m &= m_1, & \ell &= \ell_1, \\ a_j^{\mathfrak{m}} &= a_{1,j}^{\mathfrak{m}}, & b_j^{\mathfrak{m}} &= b_{1,j}^{\mathfrak{m}}, & c_j^{\mathfrak{m}} &= c_{1,j}^{\mathfrak{m}}, & a_j^{\mathfrak{l}} &= a_{1,j}^{\mathfrak{l}}, & b_j^{\mathfrak{l}} &= b_{1,j}^{\mathfrak{l}}, & c_j^{\mathfrak{l}} &= c_{1,j}^{\mathfrak{l}}, \end{aligned}$$

In this case we can take the boundary curves $(\mathfrak{m}, \mathfrak{l})$ to be a topological longitude and meridian respectively. That is, we may take \mathfrak{l} to be primitive and nullhomologous in M , and \mathfrak{m} to bound a disc in a neighbourhood of K .

We orient \mathbf{m} and \mathbf{l} so that the tangent vectors $v_{\mathbf{m}}$ and $v_{\mathbf{l}}$ to \mathbf{m} and \mathbf{l} , respectively, at the point where \mathbf{m} intersects \mathbf{l} are oriented according to the right hand rule: $v_{\mathbf{m}} \times v_{\mathbf{l}}$ points in the direction of the outward normal.

The equations (2.5)–(2.6) relating z, z', z'' variables, the gluing equations (2.11), and the cusp equations (2.13)–(2.14) are then equations in the variables z_j, z'_j, z''_j and ℓ, m . We consider solving these equations for ℓ, m , eliminating the variables z_j, z'_j, z''_j to obtain a relation between ℓ and m .

Champanerker [2] showed that the above equations can be solved in this sense to give divisors of the $\mathrm{PSL}(2, \mathbb{C})$ A-polynomial of M . Segerman showed that, if one takes a certain extended version of this variety, there exists a triangulation such that all factors of the $\mathrm{PSL}(2, \mathbb{C})$ A-polynomial are obtained [25]. See also [13] for an effective algorithm.

Theorem 2.15 (Champanerker). *When we solve the system of equations (2.5)–(2.6), (2.11) and (2.13)–(2.14) in terms of m and ℓ , we obtain a factor of the $\mathrm{PSL}(2, \mathbb{C})$ A-polynomial.*

2.3. Logarithmic equations and Neumann-Zagier matrix. We now return to the general case where the number n_c of cusps of M is arbitrary.

Note that equation (2.5) relating z_j, z'_j, z''_j , the gluing equations (2.11), and the cusp equations (2.13)–(2.14) are multiplicative. By taking logarithms now we make them additive.

Equation (2.5) implies that each z_j, z'_j and z''_j is nonzero. Taking (an appropriate branch of) a logarithm we obtain

$$\log z_j + \log z'_j + \log z''_j = i\pi$$

Define $Z_j = \log z_j$ and $Z'_j = \log z'_j$, using the branch of the logarithm with argument in $(-\pi, \pi]$, and then define Z''_j as

$$(2.16) \quad Z''_j = i\pi - Z_j - Z'_j,$$

so that indeed Z''_j is a logarithm of z''_j .

In a hyperbolic triangulation, each tetrahedron parameter has positive imaginary part. The arguments of z_j, z'_j, z''_j (i.e. the imaginary parts of Z_j, Z'_j, Z''_j) are the dihedral angles at the a -, b - and c -edges of Δ_j respectively. They are the angles of a Euclidean triangle, hence they all lie in $(0, \pi)$ and they sum to π .

The gluing equation (2.11) expresses the fact that tetrahedra fit together around an edge. Taking a logarithm, we may make the somewhat finer statement that dihedral angles around the edge sum to 2π . Thus we take the logarithmic form of the gluing equations as

$$(2.17) \quad \sum_{j=1}^n a_{k,j} Z_j + b_{k,j} Z'_j + c_{k,j} Z''_j = 2\pi i.$$

We similarly obtain logarithmic forms of the cusp equations (2.13)–(2.14) as

$$(2.18) \quad \log m_k = \sum_{j=1}^n a_{k,j}^m Z_j + b_{k,j}^m Z'_j + c_{k,j}^m Z''_j,$$

$$(2.19) \quad \log \ell_k = \sum_{j=1}^n a_{k,j}^l Z_j + b_{k,j}^l Z'_j + c_{k,j}^l Z''_j.$$

We can then observe that any solution of (2.16) and the logarithmic gluing and cusp equations (2.17)–(2.19) yields, after exponentiation, a solution of (2.5) and the original gluing (2.11) and cusp equations (2.13)–(2.14). Moreover, any solution of (2.5), (2.11) and (2.13)–(2.14) has a logarithm which is a solution of (2.16) and (2.17)–(2.19).

Using equation (2.16) we eliminate the variables Z''_j (just as using equation (2.5) we can eliminate the variables z''_j). In doing so, coefficients are combined in a way that persists throughout this paper, and so we define these combinations as follows.

Definition 2.20. For a given labelled triangulation of M , we define

$$\begin{aligned} d_{k,j} &= a_{k,j} - c_{k,j}, & d'_{k,j} &= b_{k,j} - c_{k,j}, & c_k &= \sum_{j=1}^n c_{k,j} & \text{for } k = 1, 2, \dots, n, \\ \mu_{k,j} &= a_{k,j}^m - c_{k,j}^m, & \mu'_{k,j} &= b_{k,j}^m - c_{k,j}^m, & c_k^m &= \sum_{j=1}^n c_{k,j}^m & \text{for } k = 1, 2, \dots, n_c, \\ \lambda_{k,j} &= a_{k,j}^l - c_{k,j}^l, & \lambda'_{k,j} &= b_{k,j}^l - c_{k,j}^l, & c_k^l &= \sum_{j=1}^n c_{k,j}^l & \text{for } k = 1, 2, \dots, n_c. \end{aligned}$$

Note that the index k in the first line steps through the n edges, while the index k in the next two lines steps through the n_c cusps.

When $n_c = 1$ we can drop the k subscript on cusp terms, so we have

$$\mu_j = a_j^m - c_j^m, \quad \mu'_j = b_j^m - c_j^m, \quad c^m = \sum_{j=1}^n c_j^m, \quad \lambda_j = a_j^l - c_j^l, \quad \lambda'_j = b_j^l - c_j^l, \quad c^l = \sum_{j=1}^n c_j^l.$$

We thus rewrite the the logarithmic gluing and cusp equations (2.17)–(2.19) in terms of the variables Z_j, Z'_j and ℓ_k, m_k only, as

$$(2.21) \quad \sum_{j=1}^n d_{k,j} Z_j + d'_{k,j} Z'_j = i\pi (2 - c_k)$$

$$(2.22) \quad \sum_{j=1}^n \mu_{k,j} Z_j + \mu'_{k,j} Z'_j = \log m_k - i\pi c_k^m$$

$$(2.23) \quad \sum_{j=1}^n \lambda_{k,j} Z_j + \lambda'_{k,j} Z'_j = \log \ell_k - i\pi c_k^l.$$

Define the row vectors of coefficients in equations (2.21)–(2.23) as follows:

$$\begin{aligned} R_k^G &:= (d_{k,1} \quad d'_{k,1} \quad \cdots \quad d_{k,n} \quad d'_{k,n}) \\ R_k^m &:= (\mu_{k,1} \quad \mu'_{k,1} \quad \cdots \quad \mu_{k,n} \quad \mu'_{k,n}) \\ R_k^l &:= (\lambda_{k,1} \quad \lambda'_{k,1} \quad \cdots \quad \lambda_{k,n} \quad \lambda'_{k,n}). \end{aligned}$$

So R_k^G gives the coefficients in the logarithmic gluing equation for the k th edge E_k , and R_k^m, R_k^l give respectively the coefficients in the logarithmic cusp equations for the curves \mathfrak{m}_k and \mathfrak{l}_k on the k th cusp.

When $n_c = 1$ we again drop the k subscript on cusp terms and simply write $R^m = R_k^m$ and $R^l = R_k^l$, so that $R^m = (\mu_1, \mu'_1, \dots, \mu_n, \mu'_n)$ and $R^l = (\lambda_1, \lambda'_1, \dots, \lambda_n, \lambda'_n)$.

By re-exponentiating we observe natural meanings for the new $d, d', \mu, \mu', \lambda, \lambda', c$ coefficients of Definition 2.20. The tetrahedron parameters and the holonomies m_k, ℓ_k satisfy versions of the gluing and cusp equations without any z_j'' appearing, where the d, d' variables appear as exponents in gluing equations, $\mu, \mu', \lambda, \lambda'$ variables appear as exponents in cusp equations, and the c variables determine signs:

$$\begin{aligned} \prod_{j=1}^n z_j^{d_{k,j}} (z'_j)^{d'_{k,j}} &= (-1)^{c_k} \quad \text{for } k = 1, \dots, n \text{ (indexing edges)} \\ m_k &= (-1)^{c_k^m} \prod_{j=1}^n z_j^{\mu_{k,j}} (z'_j)^{\mu'_{k,j}}, \quad \ell_k = (-1)^{c_k^l} \prod_{j=1}^n z_j^{\lambda_{k,j}} (z'_j)^{\lambda'_{k,j}} \quad \text{for } k = 1, \dots, n_c \text{ (cusps)}. \end{aligned}$$

When $n_c = 1$, the notation for cusp equations again simplifies so we have

$$m = (-1)^{c^m} \prod_{j=1}^n z_j^{\mu_j} (z'_j)^{\mu'_j}, \quad \text{and} \quad \ell = (-1)^{c^l} \prod_{j=1}^n z_j^{\lambda_j} (z'_j)^{\lambda'_j}.$$

The matrix with rows $R_1^G, \dots, R_n^G, R_1^m, R_1^l, \dots, R_{n_c}^m, R_{n_c}^l$ is called the *Neumann–Zagier matrix*, and we denote it by NZ. The first n rows correspond to the edges E_1, \dots, E_n , and the next rows come in pairs corresponding to the pairs $(\mathbf{m}_k, \mathbf{l}_k)$ of basis curves for the cusp tori $\mathbb{T}_1, \dots, \mathbb{T}_{n_c}$. The columns come in pairs corresponding to the tetrahedra $\Delta_1, \dots, \Delta_n$. Note that the data of a labelled triangulation of Definition 2.3 give us the information to write down the matrix: the edge ordering E_1, \dots, E_n orders the rows; the tetrahedron ordering $\Delta_1, \dots, \Delta_n$ orders pairs of columns; and the oriented labelling on each labelling determines each pair of columns.

$$(2.24) \quad \text{NZ} = \begin{pmatrix} R_1^G \\ \vdots \\ R_n^G \\ R_1^m \\ R_1^l \\ \vdots \\ R_{n_c}^m \\ R_{n_c}^l \end{pmatrix} = \begin{matrix} E_1 \\ \vdots \\ E_n \\ \mathbf{m}_1 \\ \mathbf{l}_1 \\ \vdots \\ \mathbf{m}_{n_c} \\ \mathbf{l}_{n_c} \end{matrix} \begin{bmatrix} \Delta_1 & \cdots & \Delta_n \\ d_{1,1} & d'_{1,1} & \cdots & d_{1,n} & d'_{1,n} \\ \vdots & \ddots & & \vdots & \\ d_{n,1} & d'_{n,1} & \cdots & d_{n,n} & d'_{n,n} \\ \mu_{1,1} & \mu'_{1,1} & \cdots & \mu_{1,n} & \mu'_{1,n} \\ \lambda_{1,1} & \lambda'_{1,1} & \cdots & \lambda_{1,n} & \lambda'_{1,n} \\ \vdots & \ddots & & \vdots & \\ \mu_{n_c,1} & \mu'_{n_c,1} & \cdots & \mu_{n_c,n} & \mu_{n_c,n} \\ \lambda_{n_c,1} & \lambda'_{n_c,1} & \cdots & \lambda_{n_c,n} & \lambda'_{n_c,n} \end{bmatrix}$$

The gluing and cusp equations can then be written as a single matrix equation, if we make the following definitions.

Definition 2.25. The *Z-vector*, *z-vector*, *H-vector* and *C-vector* are defined as

$$\begin{aligned} Z &:= (Z_1, Z'_1, \dots, Z_n, Z'_n)^T, \\ z &:= (z_1, z'_1, \dots, z_n, z'_n)^T, \\ H &:= (0, \dots, 0, \log m_1, \log \ell_1, \dots, \log m_{n_c}, \log \ell_{n_c})^T, \\ C &:= (2 - c_1, \dots, 2 - c_n, -c_1^m, -c_1^l, \dots, -c_{n_c}^m, -c_{n_c}^l)^T. \end{aligned}$$

The vector Z contains the logarithmic tetrahedral parameters; the vector H contains the cusp holonomies, and the vector C is a vector of constants derived from the gluing data, giving sign terms in exponentiated equations.

We summarise our manipulations of the various equations in the following statement.

Lemma 2.26. *Let \mathcal{T} be a labelled triangulation of M .*

(i) *The logarithmic gluing and cusp equations can be written compactly as*

$$(2.27) \quad \text{NZ} \cdot Z = H + i\pi C.$$

Precisely, the logarithmic gluing and cusp equations (2.21)–(2.23) are equivalent to (2.27).

- (ii) *After exponentiation, a solution Z of (2.27) gives a z which, together with z'_j defined by (2.5), yields a solution of the gluing equations (2.11) and cusp equations (2.13)–(2.14).*
- (iii) *Conversely, any solution (z_j, z'_j, z''_j) of (2.5), gluing equations (2.11) and cusp equations (2.13)–(2.14) yields a z with a logarithm Z satisfying (2.27)*
- (iv) *Any hyperbolic triangulation \mathcal{T} yields a Z and cusp holonomies H which satisfy (2.27).*

□

2.4. Symplectic and topological properties of the Neumann-Zagier matrix. The matrix NZ has nice symplectic properties, due to Neumann-Zagier [22], which we now recall.

First, we introduce notation for the standard symplectic structure on \mathbb{R}^{2N} , for any positive integer N . Denote by \mathbf{e}_i (resp. \mathbf{f}_i) the vector whose only nonzero entry is a 1 in the $(2i - 1)$ th coordinate (resp. $2i$ th coordinate). Dually, let x_i (resp. y_i) denote the coordinate function which returns the $(2i - 1)$ th coordinate (resp. $2i$ th coordinate). We define the standard symplectic form ω as

$$(2.28) \quad \omega = dx_1 \wedge dy_1 + \cdots + dx_N \wedge dy_N = \sum_{j=1}^N dx_j \wedge dy_j.$$

Thus, given two vectors $V = (V_1, V'_1, \dots, V_N, V'_N)$ and $W = (W_1, W'_1, \dots, W_N, W'_N)$ in \mathbb{R}^{2N} , we have

$$\omega(V, W) = \sum_{j=1}^N V_j W'_j - V'_j W_j.$$

Alternatively, $\omega(V, W) = V^T J W = (J V) \cdot W$, where J denotes multiplication by i on $\mathbb{C}^n \cong \mathbb{R}^{2n}$, i.e. $J(\mathbf{e}_i) = \mathbf{f}_i$ and $J(\mathbf{f}_i) = -\mathbf{e}_i$ (hence $J^2 = -1$), and \cdot is the standard dot product. As a matrix,

$$J = \begin{bmatrix} 0 & -1 & & & & \\ 1 & 0 & & & & \\ & & 0 & -1 & & \\ & & 1 & 0 & & \\ & & & & \ddots & \\ & & & & & 0 & -1 \\ & & & & & 1 & 0 \end{bmatrix}$$

The ordered basis $(\mathbf{e}_1, \mathbf{f}_1, \dots, \mathbf{e}_N, \mathbf{f}_N)$ forms a *standard symplectic basis*, satisfying

$$\omega(\mathbf{e}_i, \mathbf{f}_j) = \delta_{i,j}, \quad \omega(\mathbf{e}_i, \mathbf{e}_j) = 0, \quad \omega(\mathbf{f}_i, \mathbf{f}_j) = 0$$

for all $i, j \in \{1, \dots, N\}$. Any sequence of $2N$ vectors on which ω takes the same values on pairs is a *symplectic basis*.

Maps which preserve a symplectic form are called *symplectomorphisms*. We will need to use a few particular linear symplectomorphisms, which we describe now. The proof is a routine verification.

Lemma 2.29. *In the standard symplectic vector space $(\mathbb{R}^{2N}, \omega)$ as above, the following linear transformations are symplectomorphisms:*

- (i) Take $j, k \in \{1, \dots, N\}$ with $j \neq k$, and any $a \in \mathbb{R}$. Map $\mathbf{e}_j \mapsto \mathbf{e}_j + a\mathbf{f}_k$, $\mathbf{e}_k \mapsto \mathbf{e}_k + a\mathbf{f}_j$, and leave all other standard basis vectors unchanged.
- (ii) Take $j \in \{1, \dots, N\}$ and any $a \in \mathbb{R}$. Map $\mathbf{e}_j \mapsto \mathbf{e}_j + a\mathbf{f}_j$, and leave all other standard basis vectors unchanged.

□

In fact, it is not difficult to show that the linear symplectomorphisms above generate the group of linear symplectomorphisms which fix all \mathbf{f}_j . If we reorder the standard basis $(\mathbf{e}_1, \dots, \mathbf{e}_n, \mathbf{f}_1, \dots, \mathbf{f}_n)$, the symplectic matrices fixing the Lagrangian subspace spanned by the \mathbf{f}_j have matrices of the form

$$\begin{pmatrix} I & 0 \\ A & I \end{pmatrix}$$

where I is the $n \times n$ identity matrix and A is an $n \times n$ symmetric matrix. These form a group isomorphic to the group of $n \times n$ real symmetric matrices under addition.

Returning to the Neumann-Zagier matrix NZ, we observe that its row vectors lie in \mathbb{R}^{2n} , where n (as always) is the number of tetrahedra. These vectors in fact behave nicely with respect to ω .

Theorem 2.30 (Neumann–Zagier [22]). *With R_k^G, R_k^m, R_k^l and ω as above:*

- (i) *For all $j, k \in \{1, \dots, n\}$, we have $\omega(R_j^G, R_k^G) = 0$.*
- (ii) *For all $j \in \{1, \dots, n\}$ and $k \in \{1, \dots, n_c\}$, we have $\omega(R_j^G, R_k^m) = \omega(R_j^G, R_k^l) = 0$.*
- (iii) *For all $j, k \in \{1, \dots, n_c\}$, we have $\omega(R_j^m, R_k^l) = 2\delta_{jk}$.*
- (iv) *The row vectors R_1^G, \dots, R_n^G span a subspace of dimension $n - n_c$.*
- (v) *The rank of NZ is $n + n_c$.*

It will be useful to have the first $n - n_c$ rows of NZ linearly independent; we give this property a name.

Definition 2.31. A labelled triangulation of M is *acceptable* if its Neumann–Zagier matrix NZ has rows $R_1^G, \dots, R_{n-n_c}^G$ linearly independent.

In the light of theorem 2.30(iv), by relabelling edges if necessary, we can assume a labelled triangulation is acceptable.

According to theorem 2.30, the values of ω on pairs of vectors taken from the list of $n + n_c$ vectors $(R_1^G, \dots, R_{n-n_c}^G, R_1^m, \frac{1}{2}R_1^l, \dots, R_{n_c}^m, \frac{1}{2}R_{n_c}^l)$ agree with the value of ω on corresponding pairs in the list $(\mathbf{f}_1, \dots, \mathbf{f}_{n-n_c}, \mathbf{e}_{n-n_c+1}, \mathbf{f}_{n-n_c+1}, \dots, \mathbf{e}_n, \mathbf{f}_n)$. If $R_1^G, \dots, R_{n-n_c}^G$ are linearly independent, i.e. \mathcal{T} is acceptable, then there is a linear symplectomorphism sending each vector in the first list to the corresponding vector in the second.

Accordingly, as observed by Dimofte [6] the list of $n + n_c$ vectors

$$\left(R_1^G, \dots, R_{n-n_c}^G, R_1^m, \frac{1}{2}R_1^l, \dots, R_{n_c}^m, \frac{1}{2}R_{n_c}^l \right)$$

extends to a symplectic basis for \mathbb{R}^{2n} ,

$$\left(R_1^\Gamma, R_1^G, \dots, R_{n-n_c}^\Gamma, R_{n-n_c}^G, R_1^m, \frac{1}{2}R_1^l, \dots, R_{n_c}^m, \frac{1}{2}R_{n_c}^l \right),$$

with the addition of $n - n_c$ vectors, denoted $R_1^\Gamma, \dots, R_{n-n_c}^\Gamma$. Being a symplectic basis means that, in addition to the equations of Theorem 2.30(i)–(iii), we also have

$$\begin{aligned} \omega(R_j^\Gamma, R_k^\Gamma) &= 0 \quad \text{and} \quad \omega(R_j^\Gamma, R_k^G) = \delta_{j,k} \quad \text{for all } j, k \in \{1, \dots, n - n_c\}, \text{ and} \\ \omega(R_j^\Gamma, R_k^m) &= \omega(R_j^\Gamma, R_k^l) = 0 \quad \text{for all } j \in \{1, \dots, n - n_c\} \text{ and } k \in \{1, \dots, n_c\}. \end{aligned}$$

Indeed, the R_j^Γ may be found by solving the equations above: given R_k^G, R_k^m, R_k^l , we may solve successively for $R_1^\Gamma, R_2^\Gamma, \dots, R_{n-n_c}^\Gamma$. Being solutions of linear equations with rational coefficients, we can find each $R_j^\Gamma \in \mathbb{Q}^{2n}$.

Remark 2.32. Note that the R_j^Γ are not unique: there are many solutions to the above equations. Distinct solutions are related precisely by the linear symplectomorphisms of \mathbb{R}^{2n} fixing an $(n + n_c)$ -dimensional coisotropic subspace. Following the discussion after Lemma 2.29, such symplectomorphisms are naturally bijective with $(n - n_c) \times (n - n_c)$ real symmetric matrices. Hence the space of possible $(R_1^\Gamma, \dots, R_{n-n_c}^\Gamma)$ has dimension $\frac{1}{2}(n - n_c)(n - n_c + 1)$.

For $k \in \{1, \dots, n - n_c\}$, write

$$R_k^\Gamma = (f_{k,1} \quad f'_{k,1} \quad \dots \quad f_{k,n} \quad f'_{k,n}).$$

The symplectic basis $(R_1^G, R_1^\Gamma, \dots, R_{n-n_c}^G, R_{n-n_c}^\Gamma, R_1^m, \frac{1}{2}R_1^l, \dots, R_{n_c}^m, \frac{1}{2}R_{n_c}^l)$ forms the sequence of row vectors of a symplectic matrix, which we call $\text{SY} \in \mathbb{S}\text{p}(2n, \mathbb{R})$. When $n_c = 1$ we have

$$(2.33) \quad \text{SY} := \begin{pmatrix} R_1^\Gamma \\ R_1^G \\ \vdots \\ R_{n-1}^\Gamma \\ R_{n-1}^G \\ R^m \\ \frac{1}{2}R^l \end{pmatrix} = \begin{pmatrix} f_{1,1} & f'_{1,1} & f_{1,2} & f'_{1,2} & \cdots & f_{1,n} & f'_{1,n} \\ d_{1,1} & d'_{1,1} & d_{1,2} & d'_{1,2} & \cdots & d_{1,n} & d'_{1,n} \\ \vdots & \vdots & \vdots & \vdots & \ddots & \vdots & \vdots \\ f_{n-1,1} & f'_{n-1,1} & f_{n-1,2} & f'_{n-1,2} & \cdots & f_{n-1,n} & f'_{n-1,n} \\ d_{n-1,1} & d'_{n-1,1} & d_{n-1,2} & d'_{n-1,2} & \cdots & d_{n-1,n} & d'_{n-1,n} \\ \mu_1 & \mu'_1 & \mu_2 & \mu'_2 & \cdots & \mu_n & \mu'_n \\ \frac{1}{2}\lambda_1 & \frac{1}{2}\lambda'_1 & \frac{1}{2}\lambda_2 & \frac{1}{2}\lambda'_2 & \cdots & \frac{1}{2}\lambda_n & \frac{1}{2}\lambda'_n \end{pmatrix}$$

As a symplectic matrix, SY satisfies $(\text{SY})^T J (\text{SY}) = J$, and for any vectors V, W , $\omega(V, W) = \omega(\text{SY} \cdot V, \text{SY} \cdot W)$.

2.5. Linear and nonlinear equations and hyperbolic structures. The symplectic matrix SY of (2.33) shares several rows in common with NZ . We will need to rearrange rows of various matrices, and so we make the following definition.

Definition 2.34. Let A be a matrix with $n + 2n_c$ rows, denoted A_1, \dots, A_{n+2n_c} .

- (i) The submatrices A^I, A^{II}, A^{III} consist of the first $n - n_c$ rows, the next n_c rows, and the final $2n_c$ rows. That is,

$$A^I = \begin{pmatrix} A_1 \\ \vdots \\ A_{n-n_c} \end{pmatrix}, \quad A^{II} = \begin{pmatrix} A_{n-n_c+1} \\ \vdots \\ A_n \end{pmatrix}, \quad A^{III} = \begin{pmatrix} A_{n+1} \\ \vdots \\ A_{n+2n_c} \end{pmatrix}.$$

- (ii) The matrix A^\flat consists of the rows of A^I followed by the rows of A^{III} . In other words, it is the matrix of $n + n_c$ rows

$$A^\flat = \begin{pmatrix} A^I \\ A^{III} \end{pmatrix}.$$

Note that for the matrix A of Definition 2.34, every entry of A appears precisely once in precisely one of the matrices A^I, A^{II}, A^{III} :

$$A = \begin{pmatrix} A^I \\ A^{II} \\ A^{III} \end{pmatrix}.$$

This matrix A of Definition 2.34 includes the case of a $(n + 2n_c) \times 1$ matrix, i.e. a $(n + 2n_c)$ -dimensional vector.

Observe that Definition 2.34 applies to the Neumann-Zagier matrix NZ . The matrix NZ^I has rows $R_1^G, \dots, R_{n-n_c}^G$; acceptability of \mathcal{T} means these rows are linearly independent. By Theorem 2.30(i) and (iv), the rows of NZ^I form a basis of an isotropic subspace, and the rows of NZ^{II} also lie in this subspace. The matrix NZ^{III} has rows $R_1^m, R_1^l, \dots, R_{n_c}^m, R_{n_c}^l$. Theorem 2.30(iv) and (v) imply that the rows of NZ^\flat form a basis for the row space of NZ .

Similarly for the vector C of constants, we observe C^I contains the entries $(2 - c_1, \dots, 2 - c_{n-n_c})$, and C^{III} contains the entries $(-c_1^m, -c_1^l, \dots, -c_{n_c}^m, -c_{n_c}^l)$. And for the holonomy vector H , we have H^I and H^{II} are zero vectors, while H^{III} contains cusp holonomies.

The gluing equations (2.21) can be written as

$$(2.35) \quad \begin{pmatrix} \text{NZ}^I \\ \text{NZ}^{II} \end{pmatrix} \cdot Z = i\pi \begin{pmatrix} C^I \\ C^{II} \end{pmatrix}.$$

The first $n - n_c$ among these equations are given by

$$(2.36) \quad \text{NZ}^I \cdot Z = i\pi C^I.$$

We have seen that the rows of NZ^I span the rows of NZ^{II} , so knowing $NZ^I \cdot Z$ determines $NZ^{II} \cdot Z$. But it is perhaps not so clear whether $NZ^I \cdot Z = i\pi C^I$ implies that $NZ^{II} \cdot Z = i\pi C^{II}$. However, as we now show, in a hyperbolic situation this is in fact the case.

Lemma 2.37. *Suppose the triangulation \mathcal{T} has a hyperbolic structure. Then a vector $Z \in \mathbb{C}^{2n}$ satisfies equation (2.35) if and only if it satisfies equation (2.36).*

Proof. Hyperbolic structures (not necessarily complete) on M give solutions to the gluing equations $Z = (Z_1, Z'_1, \dots, Z_n, Z'_n) \in \mathbb{C}^{2n}$; hence the solution space of (2.35) is nonempty. As the equations of (2.36) are a subset of those of (2.35), the solution space of (2.36) is also nonempty.

Since both matrices $\begin{pmatrix} NZ^I \\ NZ^{II} \end{pmatrix}$ and NZ^I have rank $n - n_c$, the solution spaces of both (2.35) and (2.36) have the same dimension $2n - (n - n_c) = n + n_c$. \square

Thus, some of the gluing equations of (2.21), or equivalently of (2.35), are redundant. The same is true of the larger system (2.27). We have designed NZ^b to be a more efficient version of the Neumann-Zagier matrix, which contains only the necessary information for computing hyperbolic structures.

As discussed at the end of Section 2.1, the solution spaces of these equations do not in general coincide with spaces of hyperbolic structures. The solution space of (2.36) contains the space of hyperbolic structures on the triangulation \mathcal{T} , but is strictly larger. These equations treat Z_j and Z'_j as independent variables, but of course they are not. In a hyperbolic structure, $z_j = e^{Z_j}$ and $z'_j = e^{Z'_j}$ are related by the equations (2.6).

Indeed, the solution space of the linear equations (2.36) has dimension $n + n_c$, but then there are a further n conditions imposed by the relations $z_j + (z'_j)^{-1} - 1 = 0$ of (2.6). As discussed in the proof of [22, prop. 2.3], these n conditions are independent and the result is a variety of dimension n_c . However, as we just saw, this variety may in general contain points that do not correspond to hyperbolic tetrahedra; and moreover, it may not contain all hyperbolic structures, as not every hyperbolic structure may be able to be realised by the triangulation \mathcal{T} .

However, by Thurston's hyperbolic Dehn surgery theorem [26], the space of hyperbolic structures on M is also n_c -dimensional. So at a point of the variety defined by the linear equations (2.36) and the nonlinear equations (2.6) describing a hyperbolic structure, the variety locally coincides with the space of hyperbolic structures.

We summarise this section with the following statement.

Lemma 2.38. *Let \mathcal{T} be an acceptable hyperbolic triangulation of M .*

- (i) *The logarithmic gluing equations, expressed equivalently by (2.21) or (2.35), are equivalent to the smaller independent set of equations (2.36).*
- (ii) *The variety V defined by the solutions of these linear equations (2.36), together with the nonlinear equations (2.6), has dimension n_c . The hyperbolic structures on \mathcal{T} correspond to a subset of V . Near a point of V corresponding to a hyperbolic structure on \mathcal{T} , V parametrises hyperbolic structures on \mathcal{T} .*
- (iii) *The logarithmic gluing and cusp equations for \mathcal{T} are equivalent to*

$$(2.39) \quad NZ^b \cdot Z = H^b + i\pi C^b.$$

2.6. Symplectic change of variables. Dimofte in [6] considered using the matrix SY to *change variables* in the logarithmic gluing and cusp equations. We only need this in the one-cusped case, so in this section assume $n_c = 1$.

Assuming M is hyperbolic, by Lemma 2.38, the gluing and cusp equations are equivalent to (2.39). We observe that the rows of NZ^b are (up to a factor of $\frac{1}{2}$ in the rows R^l) a subset of the rows of SY. Indeed, SY is obtained from NZ^b by multiplying R^l rows by $\frac{1}{2}$, and inserting rows $R_1^\Gamma, \dots, R_{n-1}^\Gamma$.

In the equations of (2.39) $Z = (Z_1, Z'_1, \dots, Z_n, Z'_n)^T$ are regarded as variables, and we now change them using SY.

Definition 2.40. Given an acceptable hyperbolic triangulation \mathcal{T} and a choice of symplectic matrix SY, define the collection of variables $\Gamma = (\Gamma_1, G_1, \dots, \Gamma_{n-1}, G_{n-1}, M, \frac{1}{2}L)^T$ by $\Gamma = \text{SY} \cdot Z$.

In other words,

$$\begin{bmatrix} \Gamma_1 \\ G_1 \\ \vdots \\ \Gamma_{n-1} \\ G_{n-1} \\ M \\ \frac{1}{2}L \end{bmatrix} = \text{SY} \begin{bmatrix} Z_1 \\ Z'_1 \\ \vdots \\ Z_n \\ Z'_n \end{bmatrix} \Leftrightarrow \begin{cases} \Gamma_k = R_k^\Gamma \cdot Z, & \text{for } k \in \{1, \dots, n-1\}, \\ G_k = R_k^G \cdot Z & \text{for } k \in \{1, \dots, n-1\}, \\ M = R^m \cdot Z, & \text{and} \\ \frac{1}{2}L = \frac{1}{2}R^l \cdot Z. \end{cases}$$

Lemma 2.41. Let \mathcal{T} be an acceptable hyperbolic triangulation, and SY a matrix defining the variables Γ . Then the logarithmic gluing and cusp equations are equivalent to the equations

$$(2.42) \quad G_k = i\pi(2 - c_k), \quad M = \log m - i\pi c^m, \quad L = \log \ell - i\pi c^l.$$

Proof. The first $n-1$ rows of (2.39) express the gluing equations as $R_k^G \cdot Z = i\pi(2 - c_k)$, for $k \in \{1, \dots, n-1\}$. The remaining two rows of (2.39) express the cusp equations as $R^m \cdot Z = \log m - i\pi c^m$ and $R^l \cdot Z = \log \ell - c^l$. In the new variables, these equations are simplified. Note that the Γ_k variables do not appear in (2.39). \square

Dimofte's symplectic change of variables makes the linear gluing and cusp equations as simple as possible. However to find hyperbolic structures we still need to incorporate the nonlinear equations (2.6), and hence to write variables Z in terms of terms of the variables Γ . That is, we need to invert SY.

As SY is symplectic, $(\text{SY})^T J (\text{SY}) = J$ and so its inverse is given by $\text{SY}^{-1} = -J(\text{SY})^T J$.

$$(2.43) \quad (\text{SY})^{-1} = \begin{pmatrix} d'_{1,1} & -f'_{1,1} & \cdots & d'_{n-1,1} & -f'_{n-1,1} & \frac{1}{2}\lambda'_1 & -\mu'_1 \\ -d_{1,1} & f_{1,1} & \cdots & -d_{n-1,1} & f_{n-1,1} & -\frac{1}{2}\lambda_1 & \mu_1 \\ \vdots & \vdots & \vdots & \vdots & \vdots & \vdots & \vdots \\ d'_{1,n} & -f'_{1,n} & \cdots & d'_{n-1,n} & -f'_{n-1,n} & \frac{1}{2}\lambda'_n & -\mu'_n \\ -d_{1,n} & f_{1,n} & \cdots & -d_{n-1,n} & f_{n-1,n} & -\frac{1}{2}\lambda_n & \mu_n \end{pmatrix}$$

Thus we explicitly express the Z_j, Z'_j in terms of the variables of Γ , using $Z = (\text{SY})^{-1}\Gamma$.

$$(2.44) \quad Z_j = \sum_{k=1}^{n-1} d'_{k,j} \Gamma_k - f'_{k,j} G_k + \frac{1}{2} \lambda'_j M - \frac{1}{2} \mu'_j L$$

$$(2.45) \quad Z'_j = \sum_{k=1}^{n-1} -d_{k,j} \Gamma_k + f_{k,j} G_k - \frac{1}{2} \lambda_j M + \frac{1}{2} \mu_j L$$

2.7. Inverting without inverting. Throughout this section, we continue with the assumption $n_c = 1$.

It is possible to explicitly compute a symplectic matrix SY, then invert it, express the variables Z in terms of the variables Γ by (2.44)–(2.45), and then solve to obtain the A-polynomial. However, we now show that we can perform this calculation without ever having to find SY or its inverse SY^{-1} explicitly — *provided* that we can find a certain sign term.

To see why this should be the case, note the following preliminary observation. Equations (2.44)–(2.45) express Z_j and Z'_j in terms of the Γ_k, G_k, M and L . The coefficients of the Γ_k, M and L are

numbers which appear in the Neumann-Zagier matrix. The only coefficients which do not appear in NZ are the coefficients of the G_k . But the gluing equations (2.42) say that $G_k = i\pi(2 - c_k)$, so upon exponentiation these terms only contribute a sign. In other words, up to sign, all the information we need to write the Z_j in terms of the new variables Γ_k, G_k, L, M is already in the Neumann-Zagier matrix.

To implement this idea, observe that the matrix $-J(\text{NZ}^b)^T$ shares numerous columns with SY^{-1} :

$$(2.46) \quad (\text{NZ}^b \cdot J)^T = (-J)(\text{NZ}^b)^T = \begin{bmatrix} d'_{1,1} & d'_{2,1} & \cdots & d'_{n-1,1} & \mu'_1 & \lambda'_1 \\ -d_{1,1} & -d_{2,1} & \cdots & -d_{n-1,1} & -\mu_1 & -\lambda_1 \\ \vdots & \vdots & \ddots & \vdots & \vdots & \vdots \\ d'_{1,n} & d'_{2,n} & \cdots & d'_{n-1,n} & \mu'_n & \lambda'_n \\ -d_{1,n} & -d_{2,n} & \cdots & -d_{n-1,n} & -\mu_n & -\lambda_n \end{bmatrix}$$

In particular, for any quantities $A_1, \dots, A_{n-1}, A_\lambda, A_\mu$,

$$\begin{aligned} \text{SY}^{-1} [A_1 \ 0 \ A_2 \ 0 \ \cdots \ A_{n-1} \ 0 \ A_\lambda \ A_\mu]^T = \\ (-J)(\text{NZ}^b)^T [A_1 \ A_2 \ \cdots \ A_{n-1} \ -A_\mu \ \frac{1}{2}A_\lambda]^T \end{aligned}$$

Splitting up the Γ_k and G_k terms, using Definition 2.40 and informed by the gluing and cusp equations (2.42) setting the expressions G_k and $M - \log m$, $L - \log \ell$ equal to constants, we obtain

$$(2.47) \quad \begin{bmatrix} Z_1 \\ Z'_1 \\ \vdots \\ Z_n \\ Z'_n \end{bmatrix} = \text{SY}^{-1} \left(\begin{bmatrix} \Gamma_1 \\ 0 \\ \vdots \\ \Gamma_{n-1} \\ 0 \\ \log m \\ \frac{1}{2} \log \ell \end{bmatrix} + \begin{bmatrix} 0 \\ G_1 \\ \vdots \\ 0 \\ G_{n-1} \\ M - \log m \\ \frac{1}{2}L - \frac{1}{2} \log \ell \end{bmatrix} \right) = (-J)(\text{NZ}^b)^T \begin{bmatrix} \Gamma_1 \\ \vdots \\ \Gamma_{n-1} \\ -\frac{1}{2} \log \ell \\ \frac{1}{2} \log m \end{bmatrix} + \text{SY}^{-1} \begin{bmatrix} 0 \\ G_1 \\ \vdots \\ 0 \\ G_{n-1} \\ M - \log m \\ \frac{1}{2}L - \frac{1}{2} \log \ell \end{bmatrix}.$$

The first term of (2.47) only involves NZ. The final vector consists of the precise quantities which are fixed to be constants by the gluing and completeness equations (2.42). Indeed, (2.42) says precisely that the final vector in equation (2.47) is a vector of constants essentially identical in content to $\pi i C^b$. We define

$$C^\# = \left(0, 2 - c_1, 0, 2 - c_2, \dots, 0, 2 - c_{n-1}, -c_\mu, -\frac{1}{2}c_\lambda \right)^T,$$

which is C^b , with some zeroes inserted, and a factor of one half. So the final vector in (2.47) is set to $\pi i C^\#$, and we obtain the following.

Proposition 2.48. *Suppose \mathcal{T} is an acceptable hyperbolic triangulation and SY a matrix defining the variables Γ . Then the logarithmic gluing and cusp equations are equivalent to*

$$(2.49) \quad \begin{bmatrix} Z_1 \\ Z'_1 \\ \vdots \\ Z_n \\ Z'_n \end{bmatrix} = (-J)(\text{NZ}^b)^T \begin{bmatrix} \Gamma_1 \\ \vdots \\ \Gamma_{n-1} \\ -\frac{1}{2} \log \ell \\ \frac{1}{2} \log m \end{bmatrix} + \pi i \text{SY}^{-1} C^\#.$$

□

Once we find a vector $B = \text{SY}^{-1} C^\#$, Proposition 2.48 allows us to express the Z_j and Z'_j in terms of the variables $\Gamma_1, \dots, \Gamma_{n-1}$, and the holonomies ℓ, m of the longitude and meridian, using only

information already available in the Neumann-Zagier matrix. There is no need to find the extra vectors R_k^Γ of the symplectic basis, or the matrix SY.

If in addition B is an *integer* vector, then when we exponentiate (2.49) to obtain the tetrahedron parameters $z_j = e^{Z_j}$ and $z'_j = e^{Z'_j}$, B determines a sign. Hence we refer to this term as a sign term.

The approach outlined above may sound paradoxical: we avoid calculating the symplectic matrix SY, by finding a vector $B = SY^{-1}C^\#$. This seems to involve the symplectic matrix SY anyway! However, in the next section we show that we can find B by solving a simpler equation, involving only the Neumann-Zagier matrix, and then *choose* SY so that $B = SY^{-1}C^\#$ holds. That is, we may use the flexibility in choosing R_k^Γ of Remark 2.32 to choose SY appropriately.

2.8. The sign term. Still assuming $n_c = 1$, we now demonstrate the existence of an SY and an integer vector B satisfying $SY \cdot B = C^\#$.

The rows of the matrix equation $SY \cdot B = C^\#$ are

$$(2.50) \quad R_k^\Gamma \cdot B = 0, \quad \text{for } k = 1, \dots, n-1,$$

$$(2.51) \quad R_k^G \cdot B = 2 - c_k, \quad \text{for } k = 1, \dots, n-1,$$

$$(2.52) \quad R^m \cdot B = -c^m, \quad R^l \cdot B = -c^l.$$

Equations (2.51)–(2.52) are exactly the equations in the rows of a matrix equation with NZ^b:

$$(2.53) \quad \text{NZ}^b \cdot B = C^b.$$

This equation has been studied by Neumann; it is known to always have an integer solution.

Theorem 2.54 (Neumann [21], Theorem 2.4).

- (i) *There exists an integer vector B satisfying $\text{NZ} \cdot B = C$.*
- (ii) *Given a B_0 such that $\text{NZ} \cdot B_0 = C$, the set of all solutions to $\text{NZ} \cdot B = C$ is*

$$B_0 + \text{Span}_{\mathbb{Z}}(JR_1^G, \dots, JR_n^G) = \left\{ B_0 + \sum_{k=1}^n a_k JR_k^G \mid a_1, \dots, a_n \in \mathbb{Z} \right\}.$$

(We will not need part (ii) of the theorem until later, but we state it now.) Note that, by taking a subset of the rows, or equations, $\text{NZ} \cdot B = C$ implies $\text{NZ}^b \cdot B = C^b$.

In order to solve $SY \cdot B = C^\#$, it remains to satisfy the equations (2.50). As discussed above, we do this not by adjusting B , but by judicious choice of the vectors R_k^Γ , and hence the matrix SY. Recall from Section 2.4 that there is substantial freedom in choosing the vectors R_k^Γ . But first we deal with a technical condition on the triangulation, which we need for the argument.

Definition 2.55. A labelled triangulation \mathcal{T} of a one-cusped manifold M is *good* if it is acceptable, and there exists a $k \in \{1, \dots, n-1\}$ such that $c_k \neq 2$.

Recall $c_k = \sum_{j=1}^n c_{k,j}$ (Definition 2.20), where $c_{k,j}$ is the number of c -edges of the tetrahedron Δ_j identified to edge E_k (Definition 2.7). So c_k is just the number of c -edges of tetrahedra identified to E_k . Thus, the goodness condition requires that some edge be incident to a number of c -edges other than 2. This is not a strong requirement, as we now show.

Lemma 2.56. *Any triangulation of a one-cusped M has a labelling which is good.*

In fact, as we will see, to make a triangulation good, one can start from any labelled triangulation, and it suffices to relabel the vertices of at most one tetrahedron, and possibly reorder some edges. Moreover, we can choose any edge E_k of an acceptable triangulation with $k \in \{1, \dots, n-1\}$, and adjust so that this particular edge is incident to $c_k \neq 2$ c -edges.

Proof. Take a labelled triangulation \mathcal{T} of M ; by reordering edges if necessary, assume \mathcal{T} is acceptable. We will show that there is a relabelling of \mathcal{T} which is good.

Choose some $k \in \{1, \dots, n-1\}$. As \mathcal{T} is acceptable, the vectors R_1^G, \dots, R_{n-1}^G are linearly independent; in particular, R_k^G is nonzero. We claim that if $c_k = 2$, then \mathcal{T} can be relabelled so that $c_k \neq 2$.

Let Δ_t be a tetrahedron of \mathcal{T} . The relabellings of Δ_t have the effect of cyclically permuting the a -, b - and c -edges (see Definition 2.1 and subsequent discussion), hence cyclically permuting the triple $(a_{k,t}, b_{k,t}, c_{k,t})$; however other terms $c_{k,j}$ in the sum for c_k are unchanged. Hence, if one of $a_{k,t}$ or $b_{k,t}$ is not equal to $c_{k,t}$, then a relabelling of Δ_t will change c_k to a distinct value, hence not 2, as claimed. Otherwise, all relabellings of Δ_t leave $c_k = 2$, and we have $a_{k,t} = b_{k,t} = c_{k,t}$, hence $d_{k,t} = d'_{k,t} = 0$ (Definition 2.20).

The above argument applies to any tetrahedron Δ_t of \mathcal{T} . Thus, if every relabelling of any single tetrahedron leaves $c_k = 2$, then the numbers $d_{k,t} = d'_{k,t} = 0$ for all $t \in \{1, \dots, n-1\}$. But these are precisely the entries in the vector R_k^G forming a row of NZ^b , so $R_k^G = 0$, contradicting $R_k^G \neq 0$ above. This contradiction proves the claim.

Thus, there exists a relabelling of a single tetrahedron that makes $c_k \neq 2$. Call the resulting labelled triangulation \mathcal{T}' and Neumann-Zagier matrix NZ' . Potentially the relabelling may have the effect that NZ' no longer has its first $n-1$ row vectors linearly independent. However by Theorem 2.30(iv), the first n row vectors of NZ' span an $(n-1)$ -dimensional space. By construction the k th row R_k^G remains nonzero. Hence we may relabel the edges so that the edges labelled $1, \dots, n-1$ have linearly independent row vectors, and our chosen edge is among them. This relabelling is then good. \square

A good triangulation has the property that the vector C^b has a nonzero entry among its first $n-1$ entries. As we now see, this nonzero entry provides the leverage to make a good choice of vectors R_k^Γ forming a symplectic basis, so that they also satisfy (2.50).

Lemma 2.57. *Suppose that \mathcal{T} is a good labelled triangulation. Let $B \in \mathbb{Z}^{2n}$ be a vector satisfying $\text{NZ}^b \cdot B = C^b$. Then there exist vectors $R_1^\Gamma, \dots, R_{n-1}^\Gamma$ in \mathbb{Q}^{2n} such that*

- (i) $(R_1^\Gamma, R_1^G, \dots, R_{n-1}^\Gamma, R_{n-1}^G, R^m, \frac{1}{2}R^l)$ forms a symplectic basis, and
- (ii) for all $j \in \{1, \dots, n-1\}$ we have $R_j^\Gamma \cdot B = 0$.

Proof. We start from arbitrary choices of the $R_k^\Gamma \in \mathbb{Q}^{2n}$ such that $(R_1^\Gamma, R_1^G, \dots, R_{n-1}^\Gamma, R_{n-1}^G, R^m, \frac{1}{2}R^l)$ is a symplectic basis.

Observe that Lemma 2.29 allows us to adjust the R_k^Γ , without changing any R_k^G , R^m or R^l , so that we still have a symplectic basis. In particular, we may make the following modifications to the R_k^Γ .

- (i) Take $j, k \in \{1, \dots, n-1\}$ with $j \neq k$ and $a \in \mathbb{R}$, and map $R_j^\Gamma \mapsto R_j^\Gamma + aR_k^G$, $R_k^\Gamma \mapsto R_k^\Gamma + aR_j^G$.
- (ii) Take $j \in \{1, \dots, n-1\}$ and $a \in \mathbb{R}$, and map $R_j^\Gamma \mapsto R_j^\Gamma + aR_j^G$.

Let $R_j^\Gamma \cdot B = a_j$. We adjust the R_j^Γ until all $a_j = 0$.

We claim there exists a $k \in \{1, \dots, n-1\}$ such that $R_k^G \cdot B \neq 0$. Indeed, as \mathcal{T} is good, there exists a $k \in \{1, \dots, n-1\}$ such that $c_k \neq 2$. Then the k th row of the equation $\text{NZ}^b \cdot B = C^b$ says that $R_k^G \cdot B = 2 - c_k$, which is nonzero as claimed.

Let $\alpha = R_k^G \cdot B$, so $\alpha \neq 0$. First, we modify R_k^Γ by (ii), replacing R_k^Γ with $(R_k^\Gamma)' = R_k^\Gamma - \frac{a_k}{\alpha} R_k^G$. We then have $(R_k^\Gamma)' \cdot B = R_k^\Gamma \cdot B - \frac{a_k}{\alpha} R_k^G \cdot B = 0$. Thus the modification makes $a_k = 0$; the other a_j are unchanged.

Now consider $j \neq k$. If $R_j^G \cdot B \neq 0$ we similarly modify R_j^Γ by (ii) to set $a_j = 0$. Otherwise, $R_j^G \cdot B = 0$ and we modify R_j^Γ and R_k^Γ by (i), replacing them with $(R_j^\Gamma)' = R_j^\Gamma - \frac{a_j}{\alpha} R_k^G$ and

$(R_k^\Gamma)' = R_k^\Gamma - \frac{a_j}{\alpha} R_j^G$ respectively. We then have $(R_j^\Gamma)' \cdot B = R_j^\Gamma \cdot B - \frac{a_j}{\alpha} R_k^G \cdot B = 0$ and $(R_k^\Gamma)' \cdot B = R_k^\Gamma \cdot B - \frac{a_j}{\alpha} R_j^G \cdot B = a_k = 0$. Again the effect is to set $a_j = 0$ and leave the other a_i unchanged.

Modifying R_j^Γ in this way for each $j \neq k$, we obtain the desired vectors. \square

We summarise the result of this section in the following proposition.

Proposition 2.58. *Let \mathcal{T} be a good hyperbolic triangulation of a one-cusped M . Let B be an integer vector such that $\text{NZ}^b \cdot B = C^b$ (such a vector exists by Theorem 2.54). Then there exists a symplectic matrix SY defining variables Γ , such that the logarithmic gluing and cusp equations are equivalent to the equation*

$$(2.59) \quad \begin{bmatrix} Z_1 \\ Z_1' \\ \vdots \\ Z_n \\ Z_n' \end{bmatrix} = (-J)(\text{NZ}^b)^T \begin{bmatrix} \Gamma_1 \\ \vdots \\ \Gamma_{n-1} \\ -\frac{1}{2} \log \ell \\ \frac{1}{2} \log m \end{bmatrix} + \pi i B.$$

\square

We have now realised our claim of “inverting without inverting”. Proposition 2.58 allows us to convert the variables Z_i, Z_i' into the variables Γ_i , together with the cusp holonomies ℓ, m , without having to actually calculate the vectors R_i^Γ or the matrix SY ! The only information we need is the Neumann-Zagier matrix NZ , and the integer vector B such that $\text{NZ}^b \cdot B = C^b$.

2.9. The A-polynomial from gluing equations and from Ptolemy equations. Suppose that $n_c = 1$, we have a good labelled triangulation \mathcal{T} , and a vector $B = (B_1, B_1', \dots, B_n, B_n')^T$ such that $\text{NZ}^b \cdot B = C^b$.

Proposition 2.58 converts the logarithmic gluing and cusp equations — linear equations — into the variables $\Gamma_1, \dots, \Gamma_{n-1}$, together with the cusp holonomies m, ℓ . We now convert the nonlinear equations (2.6) into these variables.

We first convert to the exponentiated variables z_j . Let $\gamma_j = e^{\Gamma_j}$. Using equation (2.59), and the known form of $(-J)(\text{NZ}^b)^T$ from (2.46), we obtain

$$(2.60) \quad z_j = (-1)^{B_j} \ell^{-\mu_j'/2} m^{\lambda_j'/2} \prod_{k=1}^{n-1} \gamma_k^{d'_{k,j}},$$

$$(2.61) \quad z_j' = (-1)^{B_j'} \ell^{\mu_j/2} m^{-\lambda_j/2} \prod_{k=1}^{n-1} \gamma_k^{-d_{k,j}}.$$

Then the nonlinear equation (2.6) for the tetrahedron Δ_j becomes

$$(-1)^{B_j} \ell^{-\mu_j'/2} m^{\lambda_j'/2} \prod_{k=1}^{n-1} \gamma_k^{d'_{k,j}} + (-1)^{B_j'} \ell^{\mu_j/2} m^{-\lambda_j/2} \prod_{k=1}^{n-1} \gamma_k^{-d_{k,j}} - 1 = 0.$$

Since $d_{k,j} = a_{k,j} - c_{k,j}$ and $d'_{k,j} = b_{k,j} - c_{k,j}$ (Definition 2.20), we may multiply through by $\gamma^{c_{k,j}}$; then the exponents become the incidence numbers $a_{k,j}, b_{k,j}, c_{k,j}$ of the various types of edges of tetrahedra with edges of the triangulation (Definition 2.7).

$$(2.62) \quad (-1)^{B_j} \ell^{-\mu_j'/2} m^{\lambda_j'/2} \prod_{k=1}^{n-1} \gamma_k^{b_{k,j}} + (-1)^{B_j'} \ell^{\mu_j/2} m^{-\lambda_j/2} \prod_{k=1}^{n-1} \gamma_k^{a_{k,j}} - \prod_{k=1}^{n-1} \gamma_k^{c_{k,j}} = 0.$$

Each product in the above expression is simpler than it looks: it is a polynomial of total degree at most 2 in the γ_k , by Lemma 2.8! The product $\prod_{k=1}^{n-1} \gamma_k^{a_{k,j}}$ has a fixed j , referring to the specific tetrahedron Δ_j . The product is over the various edges E_k of the triangulation, with the exponent

$a_{k,j}$ being the incidence number of the a -edges of Δ_j with the edge E_k . But Δ_j only has two a -edges, so at most two of these $a_{k,j}$ are nonzero, and the $a_{k,j}$ sum to 2 as in (2.9).

Recall the notation $j(\mu\nu)$ of Definition 2.4; so for fixed j , the only nonzero $a_{k,j}$ are $a_{j(01),j}$ and $a_{j(23),j}$ (and these may be the same term). Thus the product $\prod_{k=1}^{n-1} \gamma_k^{a_{k,j}}$ is equal to the product of $\gamma_{j(01)}$ and $\gamma_{j(23)}$, with the caveat that γ_n does not appear in the product. Indeed, in Definition 2.40 we only define $\Gamma_1, \dots, \Gamma_{n-1}$, so only $\gamma_1, \dots, \gamma_{n-1}$ are defined. However, it is worthwhile to introduce γ_n as a formal variable, and then we can make the following definition.

Definition 2.63. Let \mathcal{T} be a labelled triangulation of a 3-manifold M with one cusp, and let B be an integer vector such that $\text{NZ}^b \cdot B = C^b$. The *Ptolemy equation* of the tetrahedron Δ_j is

$$(-1)^{B'_j} \ell^{-\mu_j/2} m^{\lambda_j/2} \gamma_{j(01)} \gamma_{j(23)} + (-1)^{B_j} \ell^{-\mu'_j/2} m^{\lambda'_j/2} \gamma_{j(02)} \gamma_{j(13)} - \gamma_{j(03)} \gamma_{j(12)} = 0.$$

The *Ptolemy equations* of \mathcal{T} consist of the Ptolemy equations for each tetrahedron of \mathcal{T} .

Equation (2.62) is thus the Ptolemy equation for Δ_j , with the formal variable γ_n set to 1.

Let us now put the work of this section together.

Theorem 2.64. *Let \mathcal{T} be a good hyperbolic triangulation of a one-cusped M . When we solve the system of Ptolemy equations of \mathcal{T} in terms of m and ℓ , setting $\gamma_n = 1$ and eliminating the variables $\gamma_1, \dots, \gamma_{n-1}$, we obtain a factor of the $\text{PSL}(2, \mathbb{C})$ polynomial, which is also the polynomial of Theorem 2.15.*

(Note that the polynomial described here, arising by eliminating variables from a system of equations, is only defined up to multiplication by units, and the equality of polynomials here should be interpreted accordingly.)

Proof. Theorem 2.15 tells us that solving equations (2.5)–(2.6), (2.11) and (2.13)–(2.14) for m and ℓ , eliminating the variables z_j, z'_j, z''_j , yields a factor of the $\text{PSL}(2, \mathbb{C})$ A-polynomial. By Lemma 2.26, a solution of the logarithmic gluing and cusp equations, after exponentiation, gives a solution of (2.5), (2.11) and (2.13)–(2.14); and conversely any solution of (2.5), (2.11) and (2.13)–(2.14) has a logarithm solving the logarithmic gluing and cusp equations.

By Proposition 2.58, after introducing appropriate B and SY and variables Γ , which all exist, the logarithmic gluing and cusp equations are equivalent to (2.59). Exponentiating gives us that the equations (2.60)–(2.61) imply (2.5), (2.11) and (2.13)–(2.14). Combining these with (2.6) yields the equations (2.62), one for each tetrahedron. Therefore, any solution of the equations (2.62) for $\gamma_1, \dots, \gamma_{n-1}, m, \ell$ yields a solution of (2.5)–(2.6), (2.11) and (2.13)–(2.14). Conversely, any solution of (2.5)–(2.6), (2.11) and (2.13)–(2.14) has a logarithm satisfying the logarithmic gluing and cusp equations, hence yields solutions of (2.62).

Thus the pairs (ℓ, m) arising in solutions of ((2.5)–(2.6), (2.11) and (2.13)–(2.14)) are those arising in solutions of (2.62). The latter equations are the Ptolemy equations of \mathcal{T} with γ_n set to 1. Thus, the (ℓ, m) satisfying the polynomial obtained by solving the Ptolemy equations with $\gamma_n = 1$ are also those satisfying the polynomial of Theorem 2.15. \square

Corollary 2.65. *With \mathcal{T} and M as above, letting $\mathcal{L} = \ell^{1/2}$ and $\mathcal{M} = m^{1/2}$ and solving the Ptolemy equations with $\gamma_n = 1$ as above, we obtain a polynomial in \mathcal{M} and \mathcal{L} which contains as a factor the factor of the $\text{SL}(2, \mathbb{C})$ A-polynomial describing hyperbolic structures on \mathcal{T} .*

Proof. Suppose $(\mathcal{L}, \mathcal{M})$ lies in the zero set of the factor of the $\text{SL}(2, \mathbb{C})$ A-polynomial describing hyperbolic structures on \mathcal{T} . Then there is a representation $\pi_1(M) \rightarrow \text{SL}(2, \mathbb{C})$ sending the longitude to a matrix with eigenvalues $\mathcal{L}, \mathcal{L}^{-1}$ and the meridian to a matrix with eigenvalues $\mathcal{M}, \mathcal{M}^{-1}$. Projecting to $\text{PSL}(2, \mathbb{C})$ we have the holonomy of a hyperbolic structure on \mathcal{T} whose cusp holonomies are given by $\mathcal{L}^2 = \ell$ and $\mathcal{M}^2 = m$ respectively. Hence (ℓ, m) and the tetrahedron parameters of the hyperbolic structure solve the gluing and cusp equations \mathcal{T} , hence satisfy the polynomial of Theorem 2.64. \square

3. DEHN FILLINGS AND TRIANGULATIONS

3.1. Nice triangulations of manifolds with torus boundaries. We have set up the theory for computing A-polynomials using a symplectic change of basis. One of our main applications will be adjusting A-polynomials under Dehn filling. To apply the techniques broadly, we need to show that every 3-manifold of interest admits a triangulation with nice properties. This is the purpose of this section.

Proposition 3.1. *Let \overline{M} be a connected, compact, orientable, irreducible, ∂ -irreducible 3-manifold with boundary consisting of $m + 1 \geq 2$ tori. Then, for any torus boundary component \mathbb{T}_0 , there exists an ideal triangulation \mathcal{T} of the interior M of \overline{M} such that the following hold.*

- (i) *If $\mathbb{T}_1, \dots, \mathbb{T}_m$ are the torus boundary components of \overline{M} disjoint from \mathbb{T}_0 , then in M , the cusp corresponding to \mathbb{T}_j for any $j = 1, \dots, m$ meets exactly two ideal tetrahedra, $\Delta_{j,1}$ and $\Delta_{j,2}$, meeting each tetrahedron in exactly one ideal vertex.*
- (ii) *There exists a choice of generators for $H_1(\mathbb{T}_0; \mathbb{Z})$, represented by curves \mathfrak{m}_0 and \mathfrak{l}_0 , such that \mathfrak{m}_0 and \mathfrak{l}_0 are normal with respect to the cusp triangulation inherited from \mathcal{T} , and such that \mathfrak{m}_0 and \mathfrak{l}_0 are disjoint from the tetrahedra $\Delta_{j,1}$ and $\Delta_{j,2}$, for all $j = 1, \dots, m$.*

In the notation of Section 2, the number of cusps here is $n_c = m + 1 \geq 2$.

Proof. By work of Jaco and Rubinstein [18, Prop. 5.15, Theorem 5.17], \overline{M} admits a triangulation by finite tetrahedra, i.e. with material vertices, such that the triangulation has all its vertices in $\partial\overline{M}$ and has precisely one vertex in each boundary component. Thus each component of $\partial\overline{M}$ is triangulated by exactly two material triangles.

Adjust this triangulation to a triangulation of M with ideal and material vertices, as follows. For each component of $\partial\overline{M}$, cone the boundary component to infinity. That is, attach $T^2 \times [0, \infty)$. Triangulate by coning: over the single material vertex v in \mathbb{T}_j , attach an edge with one vertex on the material vertex, and one at infinity. Over each edge e in \mathbb{T}_j , attach a $1/3$ -ideal triangle, with one side of the triangle on the edge e with two material vertices, and the other two sides on the half-infinite edges stretching to infinity. Finally, over each triangle T in \mathbb{T}_j attach a tetrahedron with one face identified to T , with all material vertices, and all other faces identified to the $1/3$ -ideal triangles lying over edges of the triangulation of $\partial\overline{M}$.

Note that each cusp of M now meets exactly two tetrahedra, in exactly one ideal vertex of each tetrahedron. To complete the proof, we need to remove material vertices.

Begin by removing a small regular neighbourhood of each material vertex; each such neighbourhood is a ball B in M . Removing B truncates the tetrahedra incident to that material vertex. We will obtain the ideal triangulation by drilling tubes from the balls to the cusp \mathbb{T}_0 , disjoint from the tetrahedra meeting the other cusps. Thus the triangulation of the distinguished cusp \mathbb{T}_0 will be affected, but the triangulations of the other cusps will remain in the form required for the result.

To drill a tube, we follow the procedure of Weeks [27] in section 3 of that paper (see also [15] figures 10 and 11 for pictures of this process). That is, truncate all ideal vertices in the triangulation of M . Truncate material vertices by removing a ball neighbourhood, giving a triangulation by truncated ideal tetrahedra of the manifold $\overline{M} - (B_0 \cup \dots \cup B_m)$ where B_0, \dots, B_m are the ball neighbourhoods of material vertices.

There exists an edge E_0 of the truncated triangulation from \mathbb{T}_0 to exactly one of the B_i ; call it B_0 . Now inductively order the B_i and choose edges E_1, \dots, E_m such that E_j has one endpoint on B_k for some $k < j$ and one endpoint on B_j . Note these edges must necessarily be disjoint from the tetrahedra meeting cusps of M disjoint from \mathbb{T}_0 , since all edges in such a tetrahedron run from a ball to a different cusp, or from a ball back to itself. Note also that such edges E_0, \dots, E_m must exist, else M is disconnected, contrary to assumption.

Starting with $i = 0$ and then repeating for each $i = 1, \dots, m$, take a triangle T_i with a side on E_i . Cut M open along the triangle T_i and insert a triangular pillow with a pre-drilled tube as in

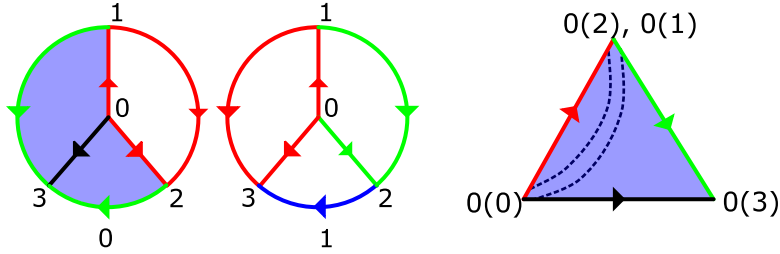


FIGURE 2. Gluing two tetrahedra as shown on the left yields a triangular pillowcase with a pre-drilled tube, as shown on the right.

	012	013	023	123
0	1 (013)	-	-	1 (012)
1	0 (123)	0 (012)	1 (123)	1 (023)

FIGURE 3. Gluing instructions to form a triangular pillow with a pre-drilled tube. Notation is as in [1].

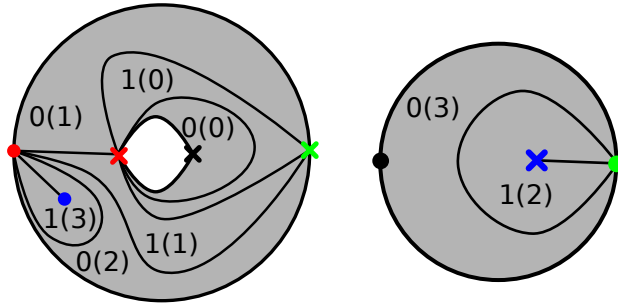


FIGURE 4. The cusp triangulations of the pillow. Each triangle in the cusp triangulation is labelled, with tetrahedron number (vertex).

[27]. The gluing of the two tetrahedra to form the tube is shown in Figure 2, with face pairings given in Figure 3. The two unglued faces are then attached to the two copies of T_i . This gives a triangulation of $\overline{M} - (B_{i+1} \cup \dots \cup B_m)$ by truncated tetrahedra, with the ball B_i merged into the boundary component corresponding to \mathbb{T}_0 . Note it only adds edges, triangles, and tetrahedra, without removing any or affecting the other edges E_j .

When we have repeated the process $m + 1$ times, we have a triangulation of \overline{M} by truncated ideal tetrahedra. By construction, each boundary component \mathbb{T}_j , $j = 1, \dots, m$, meets exactly two truncated tetrahedra $\Delta_{j,1}$ and $\Delta_{j,2}$ in exactly two ideal vertices. This gives (i).

For (ii), we trace through the gluing data in Figure 3 and Figure 2 to find the cusp triangulation of the pillow with pre-drilled tube. These are shown in Figure 4. Note there are two connected components. One is a disk made up of vertex 3 of tetrahedron 0 and vertex 2 of tetrahedron 1. The other is an annulus, made up of the remaining truncated vertices.

The cusp triangulation of the manifold $\overline{M} - (B_0 \cup \dots \cup B_m)$ consists of two triangles per torus boundary component, along with $m + 1$ triangulated 2-spheres. When we add the first pillow, we slice open a triangle, which appears in three edges of the cusp triangulation: one on the torus \mathbb{T}_0 , and the other two on the boundary of the ball B_0 . These edges of the cusp triangulation are sliced open, leaving a bigon on \mathbb{T}_0 and two bigons on B_0 . When the pillow is glued in, the bigons are

replaced. One, on the boundary of the ball B_0 , is just filled with the disk on the right of Figure 4. One on \mathbb{T}_0 is filled with the annulus on the left of Figure 4. The remaining one, on the boundary of B_0 , is glued to the inside of the annulus. Thus the cusp triangulation of \mathbb{T}_0 is changed by cutting open an edge, inserting an annulus with the triangulation on the left of Figure 4, and inserting a disk into the centre of that annulus with the (new) triangulation of the boundary of B_0 .

When we repeat this process inductively for each B_i , we slice open edges of the cusp triangulation of the adjusted \mathbb{T}_0 , and add in an annulus and disks corresponding to the triangulation of the boundary of B_i . This process only adds triangles; it does not remove or adjust existing triangles, except to separate them by inserting disks.

Now let \mathfrak{m}_0 and \mathfrak{l}_0 be any generators of $H_1(T_0; \mathbb{Z})$. We can choose representatives that are normal with respect to the triangulation of

$$\overline{M} - (B_0 \cup \cdots \cup B_m).$$

At each step, we replace an edge of the triangulation with a disk. However, note that all such disks must be contained within the centre of the first attached annulus. Now suppose \mathfrak{m}_0 runs through the edge that is replaced in the first stage. Then keep \mathfrak{m}_0 the same outside the added disk. Within the disc, let it run from one side to the other by cutting off single corners of triangles $0(2)$, $1(1)$, $1(0)$, and $0(1)$. The new curve is still a generator of homology along with \mathfrak{l}_0 . It meets the same tetrahedra as before, and the two tetrahedra added to form the tube. It does not meet any of the vertices of the tetrahedra of the ball B_0 . The curve \mathfrak{l}_0 can also be replaced in the same manner, by a curve cutting through the same cusp triangles, parallel to the segment of \mathfrak{m}_0 within these triangles. Inductively, we may replace \mathfrak{m}_0 and \mathfrak{l}_0 at each stage by curves that are identical to the previous stage, unless they meet a newly added disk, and in this case they only meet the disk in triangles corresponding to the added pillow, not in triangles corresponding to tetrahedra meeting other cusps. The result holds by induction.

Complete the proof by replacing truncated tetrahedra by ideal tetrahedra. \square

3.2. Layered solid tori. Suppose \mathfrak{c}_1 is a cusp meeting exactly two tetrahedra Δ_1^ζ and Δ_2^ζ in exactly one ideal vertex per tetrahedron, as in the construction of Proposition 3.1.

These two tetrahedra together give a triangulation of a manifold homeomorphic to $T^2 \times [0, \infty)$ with a single point removed from $T^2 \times \{0\}$. The boundary component $T^2 \times \{0\}$ of $\Delta_1^\zeta \cup \Delta_2^\zeta$ is a punctured torus, triangulated by the two ideal triangles of $\partial\Delta_1^\zeta$ and $\partial\Delta_2^\zeta$ that do not meet the cusp \mathfrak{c}_1 . We will remove $\Delta_1^\zeta \cup \Delta_2^\zeta$ from our triangulated manifold, and obtain a space with boundary a punctured torus, triangulated by the same two ideal triangles. We will then replace $\Delta_1^\zeta \cup \Delta_2^\zeta$ by a solid torus with a triangulation such that the boundary is a triangulated once-punctured torus. This will give a triangulation of the Dehn filling.

This process of triangulating a Dehn filling was first studied by Jaco and Rubinstein [17]. Our exposition is similar to that of Guéritaud and Schleimer [14].

A *layered solid torus* is a triangulation of a solid torus that was first described by Jaco and Rubinstein [17]. When working with ideal triangulations, as in our situation, the boundary of a layered solid torus consists of two ideal triangles whose union is a triangulation of a punctured torus. The space of all two-triangle triangulations of punctured tori is described by the Farey graph. A layered solid torus can be built using the combinatorics of the Farey graph.

Recall first the construction of the Farey triangulation of \mathbb{H}^2 . We view \mathbb{H}^2 in the disc model, with antipodal points $0/1$ and $1/0$ in $\partial\mathbb{H}^2$ lying on a horizontal line through the centre of the disc, and $1/1$ at the north pole, $-1/1$ at the south pole. Two points a/b and c/d in $\mathbb{Q} \cup \{\infty\} \subset \partial\mathbb{H}^2$ have distance measured by

$$\iota(a/b, c/d) = |ad - bc|.$$

Here $\iota(\cdot, \cdot)$ denotes geometric intersection number of slopes on a punctured torus. We draw an ideal geodesic between each pair $a/b, c/d$ with $|ad - bc| = 1$. This gives the *Farey triangulation*. The dual graph of the Farey triangulation is an infinite trivalent tree, which we denote by \mathcal{F} .

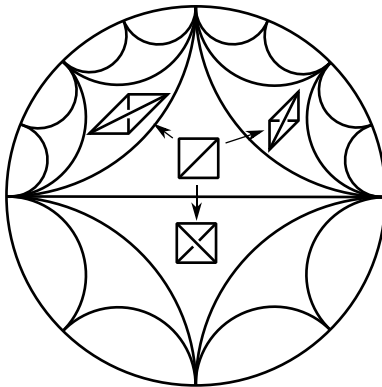


FIGURE 5. Constructing a layered solid torus

Any triangulation of a once-punctured torus consists of three slopes on the boundary of the torus, with each pair of slopes having geometric intersection number 1. Denote the slopes by f , g , h . This triple determines a triangle in the Farey triangulation. Moving across an edge (f, g) of the Farey triangulation, we arrive at another triangle whose vertices include f and g ; but the slope h is replaced with some other slope h' . This corresponds to changing the triangulation on the punctured torus, replacing lines of slope h with lines of slope h' .

In the case that we wish to perform a Dehn filling by attaching a solid torus to a triangulated once-punctured torus, there are four important slopes involved. Three of the slopes are the slopes of the initial triangulation of the once-punctured solid torus. For example, these might be $0/1$, $1/0$, and $1/1$. We will typically denote the slopes by (f, g, h) . These determine an initial triangle T_0 in the Farey graph. The other important slope is r , the slope of the Dehn filling.

Now consider the geodesic in \mathbb{H}^2 from the centre of T_0 to the slope $r \subset \partial\mathbb{H}^2$. This geodesic passes through a sequence of distinct triangles in the Farey graph, which we denote T_0, T_1, \dots, T_{N+1} . Each T_{j+1} is adjacent to T_j . We regard this as a walk or voyage through the triangulation; more precisely, we can regard T_0, \dots, T_N as forming an oriented path in the dual tree \mathcal{F} without backtracking. The slope r appears as a vertex of the final triangle T_{N+1} , but not in any earlier triangle.

We build the layered solid torus by stacking tetrahedra $\Delta_0, \Delta_1, \dots$ onto the punctured torus, replacing one set of slopes T_0 with another T_1 , then another T_2 , and so on. That is, two consecutive punctured tori always have two slopes in common and two that differ by a diagonal exchange. The diagonal exchange is obtained in three-dimensions by layering a tetrahedron onto a given punctured torus such that the diagonal on one side matches the diagonal to be replaced. See Figure 5.

For each edge crossed in the path from T_0 to T_N , layer on a tetrahedron, obtaining a collection of tetrahedra homotopy equivalent to $T^2 \times I$. After gluing k tetrahedra $\Delta_0, \dots, \Delta_{k-1}$, the side $T^2 \times \{0\}$ has the triangulation whose slopes are given by T_0 , and the side $T^2 \times \{1\}$ has slopes given by T_k . Two of the faces of Δ_{k-1} are glued to triangles of the previous layer, with slopes given by T_{k-1} , and the other two faces form a triangulation of the “top” boundary $T^2 \times \{1\}$; this triangulation has slopes given by T_k .

Continue until $k = N$, obtaining a triangulated complex consisting of N tetrahedra $\Delta_0, \dots, \Delta_{N-1}$, with boundary consisting of two once-punctured tori, one triangulated by T_0 and the other by T_N .

Recall we are trying to obtain a triangulation of a solid torus for which the slope r is homotopically trivial. Note that r is a diagonal of the triangulation T_N . That is, a single diagonal exchange replaces the triangulation T_N with T_{N+1} ; and T_{N+1} is a triangulation consisting of two slopes s and t in common with T_N , together with the slope r , which cuts across a slope r' of T_N . To homotopically kill the slope r , fold the two triangles of T_N across the diagonal slope r' , as in Figure 6. Gluing the two triangles on one boundary component of $T^2 \times I$ in this manner gives a quotient that is

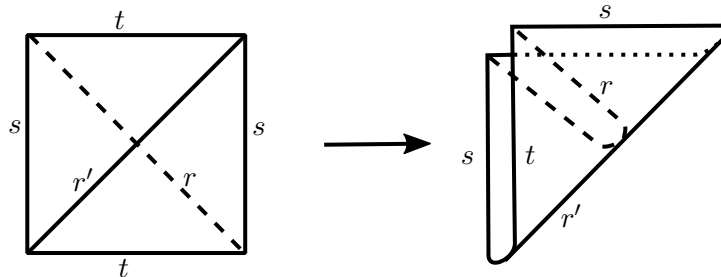


FIGURE 6. Folding makes the diagonal slope r homotopically trivial.

homeomorphic to a solid torus, with boundary still triangulated by T_0 . Inside, the slopes s and t are identified. The slope r has been folded onto itself, meaning it is now homotopically trivial. Note that N is the number of ideal tetrahedra in the layered solid torus.

Note there are two exceptional cases. If $N = 0$ then no tetrahedra are layered to form a layered solid torus. Instead, we fold across existing faces to homotopically “kill” the slope r that lies in one of the three Farey triangles adjacent to (f, g, h) . This can be considered as attaching a degenerate layered solid torus, consisting of a single face, folded into a Möbius band.

There is one other *extra-exceptional* case. In this case, the slope r is one of f, g, h . We can triangulate the Dehn filling: for example we can attach a tetrahedron covering the edge corresponding to r , performing a diagonal exchange on the once-punctured torus triangulation, then immediately fold the two new faces across the diagonal, creating an edge with valence one. This case will be ignored in the arguments below.

3.3. Notation for a voyage in the Farey triangulation. We now give notation to keep closer track of the slopes obtained at each stage of the construction of a layered solid torus.

As we have seen, each tetrahedron Δ_{k-1} replaces one set of slopes with another; the set of slopes corresponding to the triangle T_{k-1} in the Farey triangulation is replaced with the set of slopes with the triangle T_k . Thus, we associate to Δ_{k-1} an oriented edge of the dual tree \mathcal{F} of the Farey triangulation, from T_{k-1} to T_k .

As \mathcal{F} is an infinite trivalent tree, at each stage of a path in \mathcal{F} without backtracking, after we begin and before we stop, there are two choices: turning left or right. As is standard, we denote L and R for these choices. Note that the choice of L or R is not well-defined when moving from T_0 to T_1 , but thereafter the choice of L or R is well-defined. Thus, to the path T_0, T_1, \dots, T_{N+1} in \mathcal{F} , there is a word of length N in the letters $\{L, R\}$. We call this word W . The j th letter of W corresponds to the choice of L or R when moving from T_j to T_{j+1} , which also corresponds to adding tetrahedron Δ_j .

As we voyage at each stage from T_k to T_{k+1} , we pass through an edge e_k of the Farey triangulation (dual to the corresponding edge of \mathcal{F}), which has one endpoint to our left (port) and one to our right (starboard).¹ We leave behind an old slope, one of the slopes of T_k , namely the one not occurring in T_{k+1} . And we head towards a new slope, namely the slope of T_{k+1} which is not one of T_k .

Definition 3.2. As we pass from T_k to T_{k+1} , across the edge e_k , the slope corresponding to

- (i) the endpoint of e_k to our left is denoted p_k (for port);
- (ii) the endpoint of e_k to our right is denoted s_k (for starboard);
- (iii) the vertex of $T_k \setminus T_{k+1}$ is denoted o_k (old);
- (iv) the vertex of $T_{k+1} \setminus T_k$ is denoted h_k (heading).

¹As “left” and “right” are used in the context of the previous paragraph, we use the nautical terminology here.

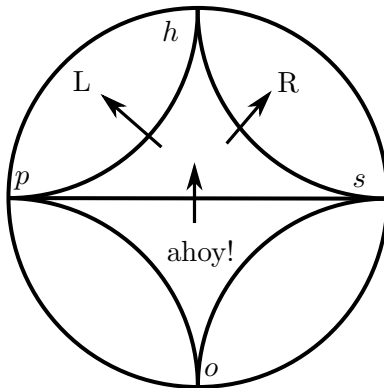


FIGURE 7. Labels on the slopes in the Farey graph.

Thus, the initial slopes $\{f, g, h\}$ are given by $\{o_0, s_0, p_0\}$ in some order, and the final, or Dehn filling slope is given by $r = h_N$. Adding the tetrahedron Δ_{k-1} , we pass from T_{k-1} to T_k , so the edges of Δ_{k-1} correspond to slopes $p_{k-1}, s_{k-1}, o_{k-1}, h_{k-1}$.

Lemma 3.3.

(i) *If the i th letter of W is an L, then*

$$o_i = s_{i-1}, \quad p_i = p_{i-1}, \quad s_i = h_{i-1}.$$

(ii) *If the i th letter of W is an R, then*

$$o_i = p_{i-1}, \quad p_i = h_{i-1}, \quad s_i = s_{i-1}.$$

Proof. This is immediate upon inspecting Figure 7. If we tack left as we proceed from T_{i-1} through T_i to T_{i+1} , then we wheel around the portside; our previous heading is now to starboard, and we leave starboard behind. Similarly for turning right. \square

So ye sail, me hearty, until ye arrive at ye last tetrahedron Δ_{N-1} , proceeding from triangle T_{N-1} into T_N , with associated slopes $o_{N-1}, s_{N-1}, h_{N-1}, p_{N-1}$. At this stage we have made $N-1$ choices of left or right, L or R. The boundary $T^2 \times \{1\}$ of the layered solid torus constructed to this point has triangulation with slopes given by T_N , i.e. with slopes $p_{N-1}, s_{N-1}, h_{N-1}$.

The final choice of L or R takes us from triangle T_N into triangle T_{N+1} , whose final heading h_N is the Dehn filling slope r .

This final L or R determines how we fold up the two triangles with slopes T_N on the boundary of Δ_N . As discussed in Section 3.2, we fold the two triangular faces of the boundary torus together along an edge, so as to make a curve of slope $r = h_N$ homotopically trivial. This means folding along the edge of slope o_N . In the process, the edges of slopes p_N and s_N are identified. An example is shown in Figure 8.

If the final, N th letter of W is an L, then $s_N = h_{N-1}$, $p_N = p_{N-1}$ and $o_N = s_{N-1}$; so we fold along the edge of slope s_{N-1} , identifying the edges of slopes h_{N-1} and p_{N-1} of the triangle T_N describing the slopes on the boundary torus after layering all the solid tori up to Δ_{N-1} .

Similarly, if the final letter of W is an R, then $s_N = s_{N-1}$, $p_N = h_{N-1}$ and $o_N = p_{N-1}$, so we fold along the edge of slope p_{N-1} , identifying the edges of slopes s_{N-1} and h_{N-1} of T_N .

3.4. Neumann-Zagier matrix of a nice triangulation. We need to describe how Dehn filling by attaching a layered solid torus affects the Neumann-Zagier matrix. This will be easiest to describe by considering the change in cusp triangulation under Dehn filling.

Start with the unfilled manifold, and assume there are $n_c \geq 2$ cusps. We consider two of these cusps $\mathfrak{c}_0, \mathfrak{c}_1$ with cusp tori $\mathbb{T}_0, \mathbb{T}_1$ respectively. We take a triangulation \mathcal{T} with the properties guaranteed by Proposition 3.1: \mathbb{T}_1 meets exactly two ideal tetrahedra Δ_1, Δ_2 , each in one ideal

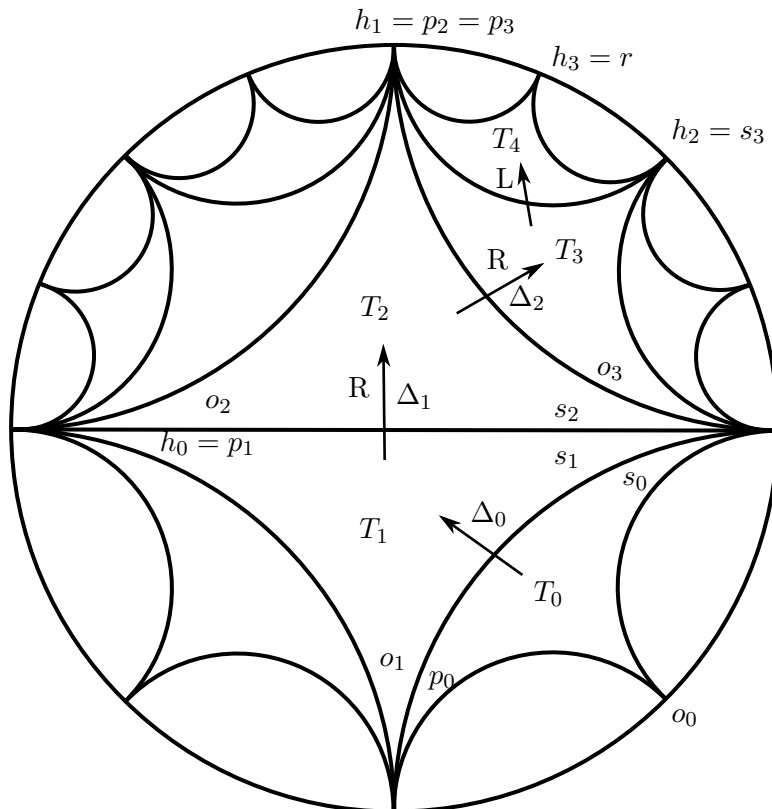


FIGURE 8. An example of a voyage in the Farey graph when $N = 3$. The word W is RRL. There are three tetrahedra added to a layered solid torus, namely Δ_0 , Δ_1 , Δ_2 . Note that slopes along the way can have several names; for example $s_0 = s_1 = s_2 = s_3$. No tetrahedron is added in the final step from T_3 to T_4 .

vertex; and we have generators $\mathfrak{m}_0, \mathfrak{l}_0$ of $H_1(\mathbb{T}_0)$ which avoid Δ_1 and Δ_2 . The cusp \mathfrak{c}_0 will remain unfilled, and cusp \mathfrak{c}_1 will be filled. There is a unique ideal edge e running into the cusp \mathfrak{c}_1 ; its other end is in \mathfrak{c}_0 . The labellings on \mathcal{T} are (at this stage) made arbitrarily.

Lemma 3.4. *Let $M, \mathcal{T}, \mathfrak{m}_0$ and \mathfrak{l}_0 be as above. There is a choice of curves $\mathfrak{m}_1, \mathfrak{l}_1$ on \mathbb{T}_1 generating $H_1(\mathbb{T}_1)$ so that the corresponding Neumann–Zagier matrix NZ has the following form.*

- (i) *The row of NZ corresponding to edge e contains only zeroes. In the cusp triangulation of \mathfrak{c}_0 , the unique vertex corresponding to e is surrounded by six triangles, corresponding to ideal vertices of Δ_1 and Δ_2 in alternating order, which form a hexagon \mathfrak{h} around e .*
- (ii) *The six vertices of \mathfrak{h} correspond to the ends of three edges of \mathcal{T} , denoted f, g, h . After possibly relabelling Δ_1 and Δ_2 , the entries of NZ in the corresponding rows, and in the columns corresponding to Δ_1, Δ_2 , are as follows.*

$$\begin{array}{c}
 \Delta_1 \qquad \Delta_2 \\
 \begin{array}{l} f \\ g \\ h \end{array} \left[\begin{array}{cc|cc} 0 & 1 & 0 & 1 \\ -1 & -1 & -1 & -1 \\ 1 & 0 & 1 & 0 \end{array} \right]
 \end{array}$$

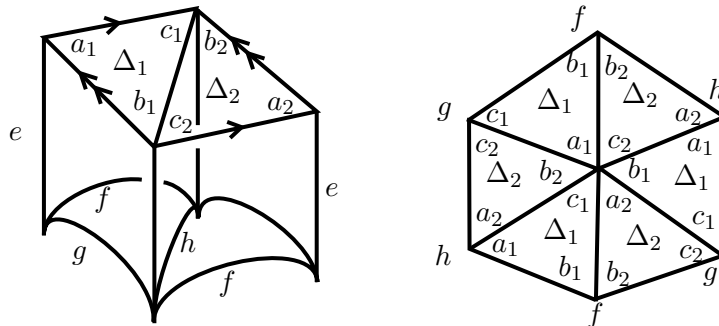


FIGURE 9. Left: How tetrahedra Δ_1 and Δ_2 meet the cusp \mathfrak{c}_1 . Right: How they meet the cusp \mathfrak{c}_0 .

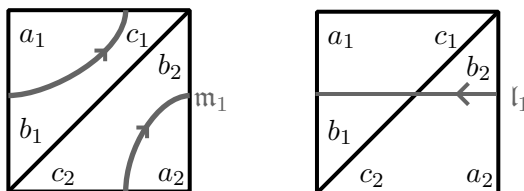


FIGURE 10. Choices for \mathfrak{m}_1 and \mathfrak{l}_1 .

- (iii) *The rows of NZ corresponding to \mathfrak{m}_1 and \mathfrak{l}_1 contain entries as shown below in the columns corresponding to Δ_1, Δ_2 , with all other entries in those rows zero.*

$$\begin{array}{c} \Delta_1 \quad \Delta_2 \\ \mathfrak{m}_1 \begin{bmatrix} 1 & 0 & -1 & 0 \end{bmatrix} \\ \mathfrak{l}_1 \begin{bmatrix} 0 & 1 & 0 & -1 \end{bmatrix} \end{array}$$

- (iv) *All other rows of NZ contain only zeroes in the columns corresponding to Δ_1 and Δ_2 .*

Proof. The proof is obtained by considering carefully the gluing. The two tetrahedra Δ_1 and Δ_2 must meet \mathfrak{c}_1 as shown in Figure 9, left. The three additional edge classes meeting these tetrahedra are labeled f , g , and h as in that figure. These three edges have both endpoints on \mathfrak{c}_0 . We may determine how they meet \mathfrak{c}_0 by tracing a curve in \mathfrak{c}_0 around the edge e . This can be done by tracing a curve around the ideal vertex of the punctured torus made up of the two faces of Δ_1 and Δ_2 that do not meet \mathfrak{c}_1 . The result is the hexagon \mathfrak{h} shown on the right of Figure 9.

Each of the eight ideal vertices of Δ_1 and Δ_2 have been accounted for: two on \mathfrak{c}_1 and six forming the hexagon \mathfrak{h} on \mathfrak{c}_0 .

Now label opposite edges of Δ_1 and Δ_2 as a -, b -, and c -edges respectively, as in Figure 9. These labels determine the 4×6 entries in the rows of the incidence matrix In , corresponding to edges e, f, g, h and tetrahedra Δ_1, Δ_2 , as follows.

$$\begin{array}{c} \Delta_1 \quad \Delta_2 \\ e \begin{bmatrix} 1 & 1 & 1 & 1 & 1 & 1 \end{bmatrix} \\ f \begin{bmatrix} 0 & 1 & 0 & 0 & 1 & 0 \end{bmatrix} \\ g \begin{bmatrix} 0 & 0 & 1 & 0 & 0 & 1 \end{bmatrix} \\ h \begin{bmatrix} 1 & 0 & 0 & 1 & 0 & 0 \end{bmatrix} \end{array}$$

As the entries in the e row account for all edges of tetrahedra incident with e , all other entries of In in this row are zero. Moreover, as the entries in the e, f, g, h rows account for all edges of Δ_1 and Δ_2 , any other row of In has all zeroes in the columns corresponding to Δ_1 and Δ_2 .

Turning to the cusp \mathfrak{c}_1 , we can choose $\mathfrak{m}_1, \mathfrak{l}_1$ as shown in Figure 10. Then \mathfrak{m}_1 has a -incidence number 1 with Δ_1 and -1 with Δ_2 (Definition 2.12), and all other incidence numbers zero. In other words, $a_{1,1}^{\mathfrak{m}} = 1$ and $a_{1,2}^{\mathfrak{m}} = -1$ are the only nonzero incidence numbers $a/b/c_{1,j}^{\mathfrak{m}}$. Similarly, \mathfrak{l}_1 has b -incidence numbers 1 with Δ_1 and -1 with Δ_2 , i.e. $b_{1,1}^{\mathfrak{l}} = 1$ and $b_{1,2}^{\mathfrak{l}} = -1$, and all other incidence numbers zero.

Forming the Neumann–Zagier matrix by subtracting columns of In , and subtracting incidence numbers, according to Definition 2.20, we obtain the form claimed in (i)–(iii).

It remains to show that in all rows of NZ other than the $e, f, g, h, \mathfrak{m}_1, \mathfrak{l}_1$ rows, there are zeroes in the Δ_1 and Δ_2 columns. We have seen that In contains only zeroes in the Δ_1 and Δ_2 columns in all rows other than e, f, g, h rows, hence NZ also has zeroes in the corresponding rows and columns. The remaining rows to consider are the \mathfrak{m}_k and \mathfrak{l}_k rows for $k = 0$ and $k \geq 2$. By construction (Proposition 3.1(ii)) $\mathfrak{m}_0, \mathfrak{l}_0$ avoid the tetrahedra Δ_1 and Δ_2 , hence the $\mathfrak{m}_0, \mathfrak{l}_0$ rows of NZ have zero in the Δ_1, Δ_2 columns. For any $k \geq 2$, the cusp \mathfrak{c}_k does not intersect Δ_1 or Δ_2 , as these tetrahedra have all their ideal vertices on \mathfrak{c}_0 and \mathfrak{c}_1 . Thus whatever curves are chosen for \mathfrak{m}_k and \mathfrak{l}_k , the corresponding rows of NZ are zero in the Δ_1 and Δ_2 columns. \square

Note that in the above proof, by relabelling the tetrahedra Δ_1, Δ_2 and cyclically permuting a -, b - and c -edges, the effect is to cyclically permute the f, g, h rows in the NZ entries above.

When we compute the Ptolemy equations for Dehn-filled manifolds, we will need a vector B as in Theorem 2.54. We now show we can obtain such a B , with properties that will be useful later.

Lemma 3.5. *Let M, \mathcal{T} , cusp curves $\mathfrak{m}_k, \mathfrak{l}_k$, tetrahedra Δ_1, Δ_2 , and the matrix NZ be as above. Suppose \mathcal{T} consists of n tetrahedra. There exists a vector $B = (B_1, B'_1, \dots, B_n, B'_n) \in \mathbb{Z}^{2n}$ with the following properties:*

- (i) $\text{NZ} \cdot B = C$;
- (ii) *The entries B_1, B'_1 and B_2, B'_2 corresponding to Δ_1 and Δ_2 are all zero.*

Proof. By Theorem 2.54(i), there exists an integer vector $A = (A_1, A'_1, \dots, A_n, A'_n)$ such that $\text{NZ} \cdot A = C$. The \mathfrak{m}_1 and \mathfrak{l}_1 rows of NZ are given by Lemma 3.4(iii), and the incidence numbers calculated in the proof show that the corresponding entries of C are $-c_1^{\mathfrak{m}} = 0$ and $-c_1^{\mathfrak{l}} = 0$. Thus the $\mathfrak{m}_1, \mathfrak{l}_1$ rows of $\text{NZ} \cdot A = C$ are $A_1 - A_2 = 0$ and $A'_1 - A'_2 = 0$. Thus we have equal pairs of integers, and the Δ_1 and Δ_2 entries of A are given by (A_1, A'_1, A_1, A'_1) .

We now adjust A to obtain the desired B , using Theorem 2.54(ii). Write R_f^G and R_h^G for the row vectors in the NZ matrix corresponding to edges f and h . Lemma 3.4(ii) says that R_f^G has $(0, 1, 0, 1)$ in the Δ_1 and Δ_2 columns, and R_h^G has $(1, 0, 1, 0)$. Thus JR_f^G has $(-1, 0, -1, 0)$ in the Δ_1 and Δ_2 columns, and JR_h^G has $(0, 1, 0, 1)$.

Now let $B = A + A_1 JR_f^G - A'_1 JR_h^G$. By Theorem 2.54(ii), $\text{NZ} \cdot B = C$, and we observe that its Δ_1, Δ_2 entries are

$$(B_1, B'_1, B_2, B'_2) = (A_1, A'_1, A_1, A'_1) + A_1(-1, 0, -1, 0) - A'_1(0, 1, 0, 1) = (0, 0, 0, 0). \quad \square$$

3.5. Neumann–Zagier matrix of a layered solid torus. Let the manifold M , triangulation \mathcal{T} , cusp curves, tetrahedra and Neumann–Zagier matrix NZ be as in the previous section.

To perform Dehn filling on \mathfrak{c}_1 , we first remove tetrahedra $\Delta_1^{\mathfrak{c}}$ and $\Delta_2^{\mathfrak{c}}$, leaving a manifold with boundary a once-punctured torus, triangulated by the boundary edges f, g , and h . Then we glue a layered solid torus to this once-punctured torus.

Because generators $\mathfrak{m}_0, \mathfrak{l}_0$ of $H_1(\mathbb{T}_0)$ were chosen to be disjoint from $\Delta_1^{\mathfrak{c}}$ and $\Delta_2^{\mathfrak{c}}$ before Dehn filling, representatives of these generators avoid the hexagon \mathfrak{h} . When we pull out $\Delta_1^{\mathfrak{c}}$ and $\Delta_2^{\mathfrak{c}}$, \mathfrak{m}_0 and \mathfrak{l}_0 still avoid \mathfrak{h} , and consequently they will form generators of $H_1(\mathbb{T}_0)$ that avoid the layered solid torus when we perform the Dehn filling.

Note that, as in Figure 9(left), the edges f, g, h are each adjacent to a unique face with an ideal vertex at \mathfrak{c}_1 . Via these faces, each of f, g, h corresponds to one of the three edges in the cusp

triangulation of \mathfrak{c}_1 , and hence to slopes on the torus \mathbb{T}_1 . As we add tetrahedra of the layered solid torus, each edge similarly corresponds to a slope on \mathbb{T}_1 . We will in fact label edges by these slopes: we denote the edge corresponding to the slope s by E_s . Thus, we regard f, g, h as slopes, and these slopes form the triangle T_0 of Section 3.2 in the Farey triangulation. In the notation of Section 3.3, $\{f, g, h\} = \{o_0, s_0, p_0\}$ in some order.

As discussed in Section 3.2, the layered solid torus that we glue is determined by the slope r of the filling, and a path in the Farey triangulation from the triangle T_0 with vertices f, g, h to the slope r . This path passes through a sequence of triangles T_0, \dots, T_{N+1} , where T_{N+1} contains r as a vertex (and previous T_j do not). The layered solid torus then contains N tetrahedra.

The j th tetrahedron (Δ_{j-1} in the notation of Section 3.3) of the layered solid torus corresponds to passing from T_{j-1} to T_j . The four vertices of these triangles are the slopes $(o_{j-1}, p_{j-1}, s_{j-1}, h_{j-1})$ as discussed in Section 3.3. Each edge of the tetrahedron corresponds to one of these four slopes. By Lemma 3.3, the sequence of “old” slopes o_0, o_1, \dots consists of distinct slopes. We will label each tetrahedron by its “old” slope: so rather than writing Δ_{j-1} , we will write $\Delta_{o_{j-1}}$.

Then in the final step we glue the two boundary faces together along the edge of slope o_N , which identifies the edges of slopes p_N and s_N . We denote this edge by $E_{p_N=s_N}$.

We arrive at an ideal triangulation of the manifold $M(r)$ obtained by Dehn filling M along slope r on cusp \mathfrak{c}_1 .

The tetrahedra of this triangulation are of two types: those inside and outside the layered solid torus. We split the columns of the Neumann-Zagier matrix into two blocks accordingly. The N tetrahedra of the layered solid torus are labelled by their “old” slopes, $\Delta_{o_0}, \dots, \Delta_{o_{N-1}}$.

The edges are of three types:

- those lying outside the layered solid torus;
- those lying on the boundary of the layered solid torus, i.e. f, g, h as above, which we call *boundary edges*; and
- (for $N \geq 1$) the edges lying in the interior of the layered solid torus, labelled by the slopes h_0, h_1, \dots, h_{N-1} .

Note that in the final folding, two of these edges are identified. Thus, the rows of the Neumann-Zagier matrix of the triangulated Dehn-filled manifold come in four blocks, corresponding to the three types of edges above, and the cusp rows for the remaining cusps \mathfrak{c}_0 and \mathfrak{c}_k for $k \geq 2$.

We regard the Dehn filled manifold $M(r)$ as built up, piece by piece, as follows. Let M_0 denote the original manifold M with the two tetrahedra Δ_1, Δ_2 removed. Let M_k denote the manifold obtained from M_0 after adding the first k tetrahedra of the layered solid torus. Thus we have

$$M_0 \subset M_1 \subset \dots \subset M_N.$$

Note M_k has a triangulation of its boundary torus with slopes (o_k, s_k, p_k) , the vertices of the triangle T_k of the Farey triangulation.

Then $M(r)$ is obtained by folding together the two boundary faces of M_n along the edge of the boundary triangulation of slope o_N , and identifying the edges of the 3-manifold triangulation of slopes s_N and p_N .

Even though each M_k is not a cusped 3-manifold, rather having boundary components, there is still a well-defined notion of labelled triangulation and incidence matrix. Moreover, since by construction the cusp curves $\mathfrak{m}_0, \mathfrak{l}_0$ avoid the removed tetrahedra Δ_1, Δ_2 , they still have well-defined incidence numbers with edges and tetrahedra. Thus there is a well-defined Neumann-Zagier matrix NZ_k for M_k , with rows for the edges and two rows for the cusp \mathfrak{c}_0 (but no rows for the boundary left behind from cusp \mathfrak{c}_1). Similarly, there is a well defined C -vector C_k for M_k (Definition 2.25).

Lemma 3.6. *The matrix NZ_0 of M_0 is obtained from the incidence matrix NZ of M by deleting the columns corresponding to the removed tetrahedra Δ_1, Δ_2 , and deleting the rows corresponding to the removed edge e and cusp \mathfrak{c}_1 .*

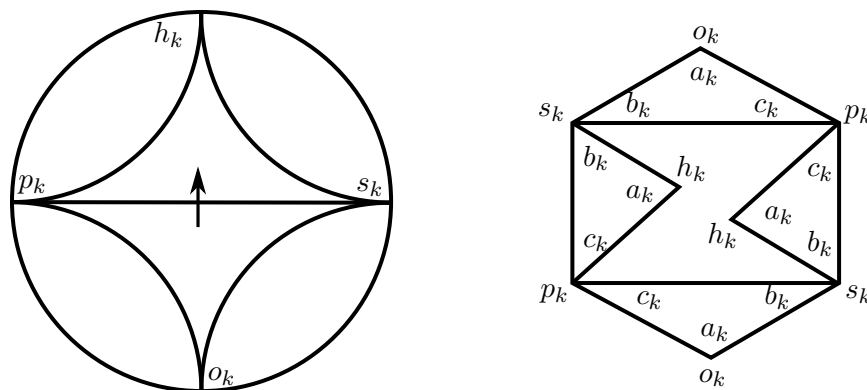


FIGURE 11. When attaching a nondegenerate layered solid torus, at each intermediate step a tetrahedron is attached with labels as shown on the right.

The vector C_0 of M_0 is obtained from the C -vector C of M by deleting the entries corresponding to edge e and the zeros corresponding to \mathfrak{m}_1 and \mathfrak{l}_1 , and adding 2 from one of the entries corresponding to edges f, g or h ; by labelling Δ_1, Δ_2 appropriately, we can specify which entry.

Proof. The deletion does not otherwise affect incidence relations, so the only effect on the Neumann-Zagier matrix is to delete entries. We similarly delete the edge e entry from C .

In Lemma 3.4, the incidence matrix entries calculated show that one edge, g , is identified with one c -edge of Δ_1 and Δ_2 , but edges f and h are not identified with any c -edges of Δ_1 or Δ_2 . Thus the g entry of C_0 is 2 greater than the g entry of C .

As noted in the comment after the proof of Lemma 3.4, by labelling Δ_1, Δ_2 appropriately, we can effectively cyclically permute the f, g, h rows, so that we add 2 to the f or h entry of C instead. \square

As each successive tetrahedron is glued, the effect on the cusp triangulation of \mathfrak{c}_0 is shown in Figure 11. The hexagon \mathfrak{h} of Lemma 3.4 has been removed, leaving a hexagonal hole; this hole is partly filled in, leaving a “smaller” hexagonal hole.

Lemma 3.7. *For an appropriate labelling of the tetrahedron Δ_{k+1} , the matrix NZ_{k+1} is obtained from NZ_k as follows.*

- (i) *Add a pair of columns for the tetrahedron Δ_{o_k} , and a row for the edge with slope h_k . All entries of the new row are zero outside of the Δ_{o_k} columns.*
- (ii) *The only nonzero entries in the Δ_{o_k} columns are in the rows corresponding to edges of slope o_k, s_k, p_k, h_k and are as follows.*

$$(3.8) \quad \begin{matrix} E_{o_k} \\ E_{p_k} \\ E_{s_k} \\ E_{h_k} \end{matrix} \begin{matrix} \Delta_{o_k} \\ \left[\begin{array}{cc} 1 & 0 \\ -2 & -2 \\ 0 & 2 \\ 1 & 0 \end{array} \right] \end{matrix},$$

- (iii) *All other entries are unchanged.*

The vector C_{k+1} is obtained from C_k by subtracting 2 from the E_{p_k} entry, and inserting an entry 2 for the row E_{h_k} .

Proof. Of the six edges of Δ_{o_k} , one of them is identified to E_{o_k} , two opposite edges are identified to E_{p_k} , two opposite edges are identified to E_{s_k} , and one is the newly added edge E_{h_k} . Observe that the three slopes of a triangle in a two-triangle triangulation of a torus are in anticlockwise order if and only if they form the vertices of a triangle of the Farey triangulation in anticlockwise order. Since (o_k, s_k, p_k) are in anticlockwise order around the triangle T_k of the Farey triangulation, they

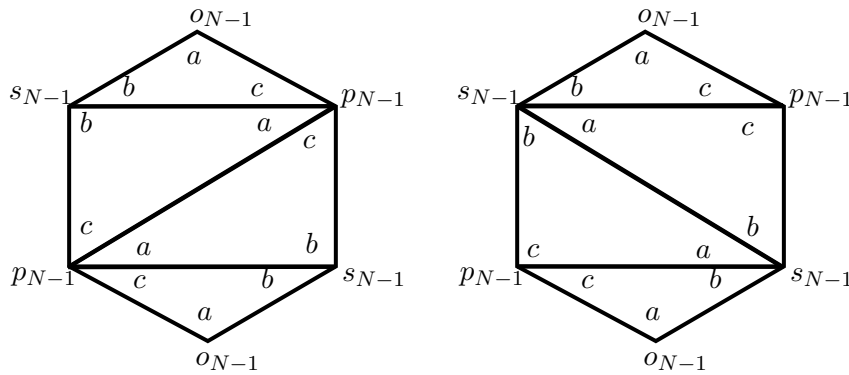


FIGURE 12. The last tetrahedron in the layered solid torus has its two interior triangles identified together, either by folding over the edge labeled p_{N-1} or by folding over the edge labeled s_{N-1} . The two cases are shown.

are slopes associated to the edges of a triangle on the boundary of M_k in anticlockwise order. Hence we may label the edges of Δ_{o_k} identified with E_{o_k} (hence also E_{h_k}) as a -edges, those identified with E_{s_k} as b -edges, and those identified with E_{p_k} as c -edges. This gives the entries of NZ_{k+1} and the changes to C -vectors claimed.

No other changes occur with incidence relations of edges and tetrahedra. As cusp curves avoid the layered solid torus, the cusp rows of the Neumann-Zagier matrix and the cusp entries of C_k are also unchanged. \square

Finally, we examine the effect of folding up the two boundary faces of M_N , and identifying the two edges E_{p_N}, E_{s_N} into an edge $E_{p_N=s_N}$ to obtain the Dehn-filled manifold $M(r)$.

We denote the row vector of NZ_N corresponding to the edge E_s of slope s by R_s^G ; and we denote the row vector of $\text{NZ}(r)$ corresponding to the identified edge $E_{p_N=s_N}$ by $R_{p_N=s_N}^G$. Similarly, we denote the entry of C_N corresponding to slope s by $(C_N)_s$; and we denote the entry of $C(r)$ corresponding to the identified edge $E_{p_N=s_N}$ by $C(r)_{p_N=s_N}$.

Lemma 3.9. *The Neumann-Zagier matrix $\text{NZ}(r)$ of $M(r)$ is obtained from NZ_N by replacing the rows corresponding to edges E_{p_N} and E_{s_N} with their sum, corresponding to the edge $E_{p_N=s_N}$.*

The C -vector $C(r)$ of $M(r)$ is obtained from C_N by replacing the entries $(C_N)_{p_N}, (C_N)_{s_N}$ corresponding to edges E_{p_N}, E_{s_N} with an entry $C(r)_{p_N=s_N} = (C_N)_{p_N} + (C_N)_{s_N} - 2$, corresponding to edge $E_{p_N=s_N}$.

Thus, the row vectors $R_{p_N}^G$ and $R_{s_N}^G$ are replaced with $R_{p_N=s_N}^G = R_{p_N}^G + R_{s_N}^G$. The corresponding entries of C_N are also summed, but then we subtract 2 for the replacement entry.

Proof. The only change in incidence relations between edges and tetrahedra after gluing is that all tetrahedra that were incident to edges E_{p_N} or E_{s_N} are now incident to the identified edge $E_{p_N=s_N}$. Thus we sum the two rows. The cusp rows are again unaffected.

Each C -vector entry corresponding to an edge E_k is of the form $2 - c_k$, where $c_k = \sum_j c_{k,j}$ (Definition 2.25). When we combine the two edges, the c_k terms combine by a sum, but in place of $2 + 2$ we must have a single 2; hence we subtract 2. \square

The effect on the cusp triangulation of \mathbf{c}_1 is to close the hexagonal hole by gluing its edges together as in Figure 12.

As mentioned previously, the slopes (p_N, s_N) are equal to (p_{N-1}, h_{N-1}) if the last letter of W is an L, and equal to (h_{N-1}, s_{N-1}) if the last letter of W is an R. Either way, we observe that the slope h_{N-1} is among those being identified. Thus the last new edge in the layered solid torus appears at step $N - 1$, with label h_{N-2} at that step.

$$\text{NZ}(r) = \begin{array}{c} \text{Edges of } M \\ \text{outside} \\ \Delta_1^\zeta \cup \Delta_2^\zeta \\ E_{o_0} \\ E_{p_0} \\ E_{s_0} \\ E_{h_0} \\ E_{h_1} \\ E_{h_2} \\ \vdots \\ E_{h_{N-2}} \\ \mathfrak{m}_0 \\ \mathfrak{l}_0 \end{array} \begin{array}{c} \text{Tet of } M \setminus (\Delta_1^\zeta \cup \Delta_2^\zeta) \\ \Delta_{o_0} \\ \Delta_{o_1} \\ \dots \\ \Delta_{o_{N-1}} \end{array} \begin{bmatrix} * & * & \cdots & * & 0 & 0 & 0 & 0 & \cdots & 0 & 0 \\ \vdots & \vdots & \ddots & \vdots & \vdots & \vdots & \vdots & \vdots & \ddots & \vdots & \vdots \\ * & * & \cdots & * & 0 & 0 & 0 & 0 & \cdots & 0 & 0 \\ * & * & \cdots & * & 1 & 0 & 0 & 0 & \cdots & 0 & 0 \\ * & * & \cdots & * & -2 & -2 & * & * & \cdots & * & * \\ * & * & \cdots & * & 0 & 2 & * & * & \cdots & * & * \\ 0 & 0 & \cdots & 0 & * & * & * & * & \cdots & * & * \\ 0 & 0 & \cdots & 0 & 0 & 0 & * & * & \cdots & * & * \\ 0 & 0 & \cdots & 0 & 0 & 0 & 0 & 0 & \cdots & * & * \\ \vdots & \vdots & \ddots & \vdots & \vdots & \vdots & \vdots & \vdots & \ddots & \vdots & \vdots \\ 0 & 0 & \cdots & 0 & 0 & 0 & 0 & 0 & \cdots & * & * \\ * & * & \cdots & * & 0 & 0 & 0 & 0 & \cdots & 0 & 0 \\ * & * & \cdots & * & 0 & 0 & 0 & 0 & \cdots & 0 & 0 \end{bmatrix}.$$

FIGURE 13. Neumann-Zagier matrix of a Dehn-filled manifold.

Alternatively, we may write the matrix $\text{NZ}(r)$ by deleting the row $E_{h_{N-1}}$ from NZ_N and adding it to the row $E_{p_{N-1}}$ or $E_{s_{N-1}}$ accordingly as the last choice is an L or R. Then the edges are regarded as having slopes $\{f, g, h\} = \{o_0, p_0, s_0\}$, together with h_0, h_1, \dots, h_{N-2} .

With this notation, the Neumann-Zagier matrix $\text{NZ}(r)$ has pairs of columns corresponding to tetrahedra, which consist of the tetrahedra of $M \setminus (\Delta_1^\zeta \cup \Delta_2^\zeta)$, and the tetrahedra of the layered solid torus, $\Delta_{o_0}, \dots, \Delta_{o_{N-1}}$. The rows correspond to the edges of M disjoint from Δ_1^ζ and Δ_2^ζ , and then edges $E_{o_0}, E_{s_0}, E_{p_0}$ on the boundary of the hexagon, then $E_{h_0}, E_{h_1}, \dots, E_{h_{N-2}}$ inside the layered solid torus; and cusp rows corresponding to $\mathfrak{m}_0, \mathfrak{l}_0$. The general form is shown in Figure 13.

Thus, if there are n edges and tetrahedra in the triangulation, then there are $n - N$ tetrahedra outside the layered solid torus, and $n - N - 2$ edges outside the layered solid torus.

Lemma 3.9 includes the case where $N = 0$, i.e. where the layered solid torus is *degenerate*. In this case we go directly from M to M_0 (removing $\Delta_1^\zeta \cup \Delta_2^\zeta$) to $M(r)$. In this case the filling slope r is equal to h_0 , so has distance 1 from two of the initial slopes f, g, h , and distance 2 from the other. These are the slopes labeled r_1, r_2 , and r_3 in Figure 14, left. No tetrahedra are added, and we skip to the final folding step, folding boundary faces of the boundary torus together along the edge of slope o_0 , and identifying the edges corresponding to slopes s_0 and p_0 . The effect is to combine and sum the rows of NZ_0 corresponding to E_{s_0} and E_{p_0} .

The resulting matrix $\text{NZ}(r)$ is described explicitly in the following propositions; they simply describe the result of applying the previous lemmas, and their proofs are immediate from those lemmas. Figure 13 shows most of the structure described.

The first proposition describes the rows corresponding to the edges outside the layered solid torus, and the cusp rows.

Proposition 3.10. *Suppose $\text{NZ}(r)$ is the Neumann-Zagier matrix of $M(r)$, obtained by Dehn filling the manifold M of Lemma 3.4, with Neumann-Zagier matrix NZ , along the slope r on \mathfrak{c}_1 . Then the rows of $\text{NZ}(r)$ corresponding to edges outside the layered solid torus and its boundary, and the rows corresponding to \mathfrak{m}_0 and \mathfrak{l}_0 , are as follows.*

- (i) *Entries in columns corresponding to the tetrahedra of the layered solid torus are all zeroes.*
- (ii) *Entries in columns corresponding to tetrahedra outside the layered solid torus are unchanged from their entries in NZ .* □

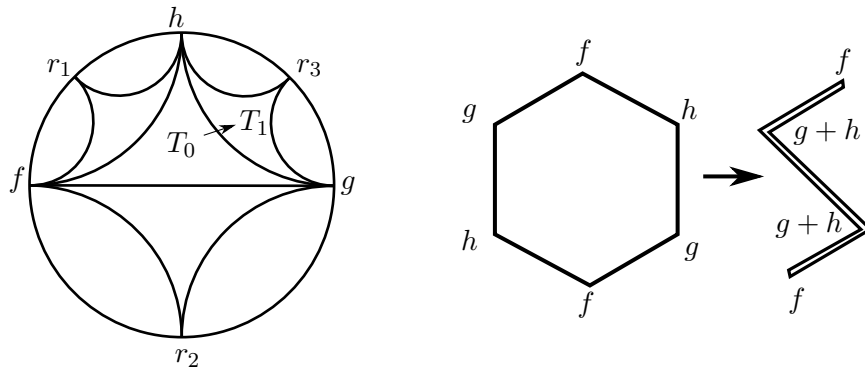


FIGURE 14. Left: Dehn filling along slope r_1 , r_2 , or r_3 attaches a degenerate layered solid torus, with no tetrahedra. Right: The effect of such a Dehn filling on the cusp triangulation of C_0 is to fold the hexagon, identifying two boundary edges together.

The remaining two propositions describe the rows of $\text{NZ}(r)$ corresponding to edges of the layered solid torus. We describe the degenerate case $N = 0$, then the generic case $N \geq 1$.

In the $N = 0$ case, by Lemma 3.9 and subsequent discussion, the only edge rows of the layered solid torus are those with slopes o_0 and $s_0 = p_0$, and there are no columns corresponding to tetrahedra in the layered solid torus.

Proposition 3.11. *Suppose $N = 0$. Then the entries in the rows of $\text{NZ}(r)$ corresponding to the edges of the layered solid torus are as follows.*

- (i) *The row corresponding to o_0 has the same entries as in the corresponding columns of NZ .*
- (ii) *The row corresponding to $s_0 = p_0$ is the sum of entries in the s_0 and p_0 rows of NZ . \square*

Proposition 3.12. *Suppose $N \geq 1$. The entries in the rows of $\text{NZ}(r)$ corresponding to the edges of the layered solid torus are as follows.*

- (i) *In columns corresponding to the tetrahedra outside the layered solid torus:*
 - (a) *the entries in the rows corresponding to the edges with slopes h_0, \dots, h_{N-2} are all zero (there are no such edges if $N = 1$); and*
 - (b) *the entries in the rows corresponding to the boundary edges, with slopes $\{f, g, h\} = \{o_0, p_0, s_0\}$ are the same as in the corresponding rows and columns of NZ . (The p_0 or s_0 row may be combined and summed with the h_{N-1} row in the final step, but being summed with zeroes, the entries remain the same.)*
- (ii) *The entries in the pair of columns corresponding to the tetrahedron Δ_{o_j} , are as described in Lemma 3.7, except that rows corresponding to slopes p_N and s_N are summed as in lemma Lemma 3.9. In particular, we have the following.*
 - (a) *The row of slope o_0 has a $(1, 0)$ in the Δ_{o_0} columns, and zeroes in every other Δ_{o_j} column.*
 - (b) *Provided $p_0 \neq p_N$, the row of slope p_0 has a sequence of pairs $(-2, -2)$, followed by $(1, 0)$ and then all zeroes. (The number of such pairs is $k + 1$, where W begins with a string of k Ls.)*
 - (c) *Provided $s_0 \neq s_N$, the row of slope s_0 has a sequence of pairs $(0, 2)$, followed by $(1, 0)$ and then all zeroes. (The number of such pairs is $k + 1$, where W begins with a string of k Rs.)*
 - (d) *In the pair of columns for Δ_{o_j} , entries in rows of slope h_{j+1}, \dots, h_{N-2} are all zeroes. \square*

3.6. Building up the sign vector. We will now show how to build up a vector $B(r)$ satisfying the sign equation (2.53) for the Dehn-filled manifold $M(r)$, that is,

$$\text{NZ}(r) \cdot B(r) = C(r).$$

We do this starting from the sign vector B found for the unfilled manifold M in Lemma 3.5. We build up a sequence of vectors B_0, \dots, B_N associated to the manifolds M_0, \dots, M_N . These vectors “almost” satisfy $\text{NZ}_k \cdot B_k = C_k$. From B_N we obtain the desired vector $B(r)$.

In Lemma 3.6, we showed that we can take C_0 to be obtained from C by deleting the e entry, and adding 2 to one of the entries corresponding to slopes $\{f, g, h\} = \{o_0, s_0, p_0\}$, whichever we prefer. For the following, we want the 2 to be added to the entry corresponding to slope s_0 or p_0 . For definiteness, we take C_0 to be obtained by adding 2 to the p_0 entry.

Lemma 3.13. *Let B_0 be the vector obtained from B by removing the two pairs of entries corresponding to the removed tetrahedra Δ_1^i, Δ_2^i . Then $C_0 - \text{NZ}_0 \cdot B_0$ consists of all zeroes, except for a 2 in the entry corresponding to the edge with slope p_0 .*

Proof. We have $\text{NZ} \cdot B = C$; examine the effect of changing the terms to $\text{NZ}_0 \cdot B_0$ and C_0 . By Lemma 3.5, the vector B has pairs of entries corresponding to Δ_1^i and Δ_2^i consisting of all zeroes.

Consider the rows of NZ corresponding to edges away from Δ_1^i and Δ_2^i , together with the $\mathbf{m}_0, \mathbf{l}_0$ rows. These rows have all zero entries in Δ_1^i and Δ_2^i columns, by Lemma 3.4. The corresponding rows of NZ_0 are obtained by deleting the zero entries in the Δ_1^i and Δ_2^i columns (Lemma 3.6). Thus the corresponding entries of $\text{NZ} \cdot B$ and $\text{NZ}_0 \cdot B_0$ are equal. Similarly, the corresponding entries of C and C_0 are equal. So $C_0 - \text{NZ}_0 \cdot B_0$ has zeroes in these entries.

By Lemma 3.6, the only remaining rows of NZ_0 are those corresponding to rows with slopes $\{f, g, h\} = \{o_0, s_0, p_0\}$.

In both $\text{NZ} \cdot B$ and $\text{NZ}_0 \cdot B_0$ we obtain exactly the same terms from the tetrahedra outside Δ_1^i and Δ_2^i , by Lemma 3.6 and construction of B_0 . These account for all the terms in $\text{NZ}_0 \cdot B_0$, but in $\text{NZ} \cdot B$ there are also terms from the tetrahedra Δ_1^i and Δ_2^i . However, as the corresponding entries of B are zero, these terms are zero. So $\text{NZ}_0 \cdot B_0$ and $\text{NZ} \cdot B$ have the same entries in these rows, and hence also C . However, as discussed above, we have chosen C_0 to differ from C by 2 in the row with slope p_0 . Hence $C_0 - \text{NZ}_0 \cdot B_0$ is as claimed. \square

It’s clear from the proof that Lemma 3.13 works equally well with the slope p_0 replaced with any of $\{f, g, h\} = \{o_0, s_0, p_0\}$.

As it turns out, going from B_0 to B_1 is a little different from the general case, and so we deal with it separately.

Lemma 3.14. *Let B_1 be obtained from B_0 by adding zero entries corresponding to the tetrahedron Δ_{o_0} . Then $C_1 - \text{NZ}_1 \cdot B_1$ consists of all zeroes, except for a 2 in the new entry corresponding to E_{h_0} .*

Proof. Recall from Lemma 3.7 that NZ_1 is obtained from NZ_0 by adding a row for the edge with slope h_0 and a pair of columns for Δ_{o_0} , with added nonzero entries as in (3.8). Moreover, C_1 is obtained from C_0 by subtracting 2 from the E_{p_0} entry, and inserting an entry 2 for the row E_{h_0} .

Now each entry of $\text{NZ}_0 \cdot B_0$ is equal to the corresponding entry in $\text{NZ}_1 \cdot B_1$, since the terms are exactly the same, except for the terms of $\text{NZ}_1 \cdot B_1$ corresponding to the added tetrahedron Δ_{o_0} , which are zero since B_1 has zero entries there. The extra entry in $\text{NZ}_1 \cdot B_1$, corresponding to E_{h_0} , is also zero, since this row of NZ_1 only has nonzero entries in the terms corresponding to Δ_{o_0} , where B_1 is zero. Thus $\text{NZ}_1 \cdot B_1$ is equal to $\text{NZ}_0 \cdot B_0$ with a 0 appended.

Similarly, each entry of C_0 is equal to the corresponding entry of C_1 , except for the entry of slope p_0 , where $C_1 - C_0$ has a -2 . The vector C_1 also has a 2 appended.

From Lemma 3.13, each entry of $C_0 - \text{NZ}_0 \cdot B_0$ is zero, except for the p_0 entry, which is 2.

Putting these together, each entry of $C_0 - \text{NZ}_0 \cdot B_0$ equals the corresponding entry of $C_1 - \text{NZ}_1 \cdot B_1$, except for the entry of slope p_0 , where $C_1 - \text{NZ}_1 \cdot B_1$ has entry $2 - 2 = 0$. The additional entry of $C_1 - \text{NZ}_1 \cdot B_1$ of slope h_0 is $2 - 0 = 2$. Thus $C_1 - \text{NZ}_1 \cdot B_1$ has the claimed form. \square

Had we chosen C_0 to differ from C in the s_0 entry, then $C_0 - \text{NZ}_0 \cdot B_0$ would have a nonzero entry for slope s_0 ; in this case we could take B_1 to be obtained from B_0 by adding entries $(0, 1)$ and obtain the same conclusion.

We now proceed to the general case, building B_{k+1} from B_k . We use the first $N - 1$ letters of the word W in the letters $\{\text{L}, \text{R}\}$.

Lemma 3.15. *Suppose $1 \leq k \leq N - 1$. If the k th letter of the word W is L (resp. R), let B_{k+1} be obtained from B_k by appending $(0, 1)$ (resp. $(0, 0)$) for the added tetrahedron Δ_{o_k} .*

Then $C_{k+1} - \text{NZ}_{k+1} \cdot B_{k+1}$ consists of all zeroes, except for a 2 in the entry corresponding to E_{h_k} .

Proof. Proof by induction on k ; Lemma 3.14 provides the base case. Assume $C_k - \text{NZ}_k \cdot B_k$ has only nonzero entry 2 in the row of slope h_{k-1} , and we consider $C_{k+1} - \text{NZ}_{k+1} \cdot B_{k+1}$.

Again using Lemma 3.7, C_{k+1} and C_k differ only in that C_{k+1} has a 2 in the new entry E_{h_k} , and has 2 subtracted from the E_{p_k} entry.

Suppose that the k th letter of W is an L. Then by Lemma 3.3 we have $o_k = s_{k-1}$, $p_k = p_{k-1}$ and $s_k = h_{k-1}$. Thus the new entries in NZ_{k+1} are given by

$$\begin{array}{l} E_{o_k} = E_{s_{k-1}} \\ E_{p_k} = E_{p_{k-1}} \\ E_{s_k} = E_{h_{k-1}} \\ E_{h_k} \end{array} \begin{array}{c} \Delta_{o_k} \\ \left[\begin{array}{cc} 1 & 0 \\ -2 & -2 \\ 0 & 2 \\ 1 & 0 \end{array} \right] \end{array}.$$

So with B_{k+1} defined as stated, the entries of $\text{NZ}_k \cdot B_k$ differ from the corresponding entries of $\text{NZ}_{k+1} \cdot B_{k+1}$ in entries for rows of slope $s_k = h_{k-1}$ and p_k . In the row of slope $s_k = h_{k-1}$, $\text{NZ}_{k+1} \cdot B_{k+1}$ is greater by 2, and in the row of slope p_k , $\text{NZ}_{k+1} \cdot B_{k+1}$ is lesser by 2. The new entry in $\text{NZ}_{k+1} \cdot B_{k+1}$ of slope h_k is 0.

Putting the above together, we find that $C_{k+1} - \text{NZ}_{k+1} \cdot B_{k+1}$ has the same entries as $C_k - \text{NZ}_k \cdot B_k$, except in the rows of slope: $s_k = h_{k-1}$, where they differ by -2 ; $p_k = p_{k-1}$, where they differ by $(-2) - (-2) = 0$; and h_k , where there is an extra entry of 2. Thus $C_{k+1} - \text{NZ}_{k+1} \cdot B_{k+1}$ has unique nonzero entry 2 in the E_{h_k} entry as desired.

Suppose that the k th letter is an R; then we have $p_i = h_{i-1}$. The argument is simpler since B_{k+1} simply appends zeroes to B_k . As we only append zeroes, there is no need to consider the new columns of NZ_{k+1} in any detail. Indeed, $\text{NZ}_{k+1} \cdot B_{k+1}$ and $\text{NZ}_k \cdot B_k$ have the same nonzero entries. Thus the nonzero entries in $C_{k+1} - \text{NZ}_{k+1} \cdot B_{k+1}$ are those of $C_k - \text{NZ}_k \cdot B_k$, with -2 added to the $p_k = h_{k-1}$ entry, and 2 inserted in the h_k entry, which gives the desired result. \square

We now consider the final step: the desired sign vector $B(r)$ is just B_N .

Lemma 3.16. *The vector B_N of Lemma 3.15 satisfies $\text{NZ}(r) \cdot B_N = C(r)$.*

Proof. By Lemma 3.9, $\text{NZ}(r)$ is obtained from NZ_n by replacing the rows of slope p_N and s_N with their sum, corresponding to the identified edge $E_{p_N=s_N}$. The row vectors $R_{p_N}^G$ and $R_{s_N}^G$ are replaced with

$$R_{p_N=s_N}^G = R_{p_N}^G + R_{s_N}^G.$$

Similarly, $C(r)$ is obtained from C_N by replacing the corresponding entries $(C_N)_{p_N}$, $(C_N)_{s_N}$ with the combined entry

$$C(r)_{p_N=s_N} = (C_N)_{p_N} + (C_N)_{s_N} - 2.$$

By Lemma 3.15, $C_N - \text{NZ}_N \cdot B_N$ has only nonzero entry 2 corresponding to slope h_{N-1} . Note that h_{N-1} is equal to one of the slopes p_N, s_N to be combined (accordingly as the final letter of W is an L or R).

Consider any row other than those corresponding to slopes p_N or s_N . Such a row is unaffected by the combination of rows or entries. Hence $C_N - \text{NZ}_N \cdot B_N$ has zero entry in this row; and since

$NZ(r)$ and $C(r)$ are equal to NZ_N and C_N in these rows, $C(r) - NZ(r) \cdot B_N$ has zero entry in these rows.

It remains to consider the single row obtained by combining two rows. Since these two rows include the row of slope h_{N-1} , the two corresponding entries of $C_N - NZ_N \cdot B_N$ are 0 and 2 in some order. These entries are $(C_N)_{p_N} - R_{p_N}^G \cdot B_N$ and $(C_N)_{s_N} - R_{s_N}^G \cdot B_N$, so

$$(C_N)_{p_N} - R_{p_N}^G \cdot B_N + (C_N)_{s_N} - R_{s_N}^G \cdot B_N = 2.$$

Putting these together, we obtain the remaining entry of $C(r) - NZ(r) \cdot B_N$ as

$$\begin{aligned} C(r)_{p_N=s_N} - R_{p_N=s_N}^G \cdot B_N &= (C_N)_{p_N} + (C_N)_{s_N} - 2 - (R_{p_N}^G + R_{s_N}^G) \cdot B_N \\ &= (C_N)_{p_N} - R_{p_N}^G \cdot B_N + (C_N)_{s_N} - R_{s_N}^G \cdot B_N - 2 = 0. \quad \square \end{aligned}$$

We have now proved the following.

Proposition 3.17. *There exists an integer vector $B(r)$ such that $NZ(r) \cdot B(r) = C(r)$. The vector $B(r)$ is given by taking a vector B for the unfilled manifold M as in Lemma 3.5, removing the two pairs of zeroes corresponding to removed tetrahedra Δ_1^c, Δ_2^c , and then appending:*

- (i) a $(0, 0)$ corresponding to the tetrahedron Δ_{o_0} ; then
- (ii) $N - 1$ pairs $(0, 1)$ or $(0, 0)$, corresponding to the first $N - 1$ letters of the word W . For each L we append a $(0, 1)$, and for each R we append a $(0, 0)$. \square

In other words, the entry of B corresponding to the tetrahedron Δ_{o_k} , for $1 \leq k \leq N - 1$, is $(0, 1)$ if the k th letter of W is an L , and $(0, 0)$ if the k th letter of W is an R .

3.7. Ptolemy equations in a layered solid torus. We can now write down explicitly the Ptolemy equations for the tetrahedra of a layered solid torus.

Theorem 3.18. *With the labelled triangulation and B -vector for the Dehn-filled manifold $M(r)$ as discussed above, the Ptolemy equations for the tetrahedra of the layered solid torus are, for $0 \leq k \leq N - 1$,*

$$\begin{aligned} -\gamma_{o_k} \gamma_{h_k} + \gamma_{s_k}^2 - \gamma_{p_k}^2 &= 0 \quad \text{if } k > 0 \text{ and the } k\text{th letter of } W \text{ is an } L, \\ \gamma_{o_k} \gamma_{h_k} + \gamma_{s_k}^2 - \gamma_{p_k}^2 &= 0 \quad \text{if } k = 0 \text{ or the } k\text{th letter of } W \text{ is an } R. \end{aligned}$$

We also set $\gamma_{p_N} = \gamma_{s_N}$.

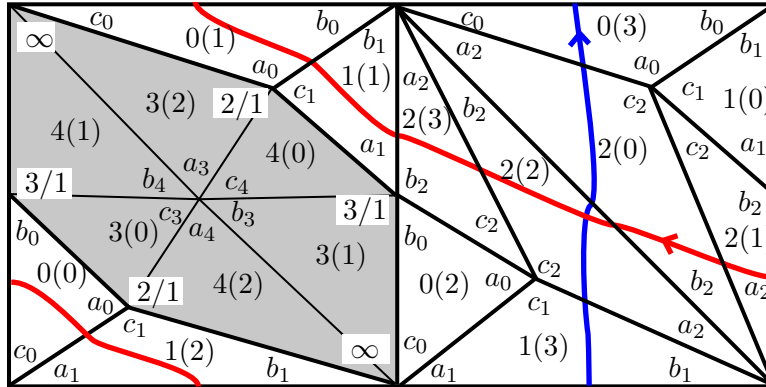
Proof. The tetrahedron Δ_{o_k} has its a -edges identified to the edges E_{o_k} and E_{h_k} , both its b -edges identified to E_{s_k} , and both its c -edges identified to E_{p_k} , so the powers of γ variables are as claimed. They are disjoint from the cusp curves $\mathfrak{m}, \mathfrak{l}$, so no powers of ℓ or m appear in the Ptolemy equations. The corresponding pair of entries of B is $(0, 0)$ for $k = 0$, and for $k \geq 1$, they are given by $(0, 1)$ if the k th letter of W is an L , and $(0, 0)$ if the k th letter of W is an R . At the final step the edges with slopes p_N and s_N are identified, with the effect of summing the corresponding rows of NZ matrices; this is also the effect of setting the variables $\gamma_{p_N}, \gamma_{s_N}$ equal in Ptolemy equations. Hence the Ptolemy equation of Definition 2.63 takes the claimed form. \square

4. EXAMPLES: DEHN-FILLING THE WHITEHEAD LINK

In this section, we work through the example of the Whitehead link and its Dehn fillings. The standard triangulation of the Whitehead link has four tetrahedra meeting each cusp. To apply our results, we need a triangulation with two tetrahedra meeting one of the cusps. This is obtained by a triangulation with five tetrahedra. Its gluing information is shown in Figure 15, where the notation is as in Regina [1]: tetrahedra are labeled by numbers 0 through 4, with vertices labeled 0 through 3. Thus faces are determined by three labels. The notation 3(021) in row 0 under column ‘‘Face 012’’ means that the face of tetrahedron 0 with vertices 012 is glued to the face of tetrahedron 3

Tetrahedron	Face 012	Face 013	Face 023	Face 123
0	3(021)	1(213)	2(130)	1(230)
1	4(102)	2(132)	0(312)	0(103)
2	2(203)	0(302)	2(102)	1(031)
3	0(021)	4(103)	4(203)	4(213)
4	1(102)	3(103)	3(203)	3(213)

FIGURE 15. Five tetrahedra triangulation of the Whitehead link complement.

FIGURE 16. Cusp triangulation of the Whitehead link, with triangles corresponding to tetrahedra 3 and 4 shaded. The edge e is at the centre of the hexagon, edges with slopes $\infty = 1/0$, $3/1$, $2/1$ on the boundary of the hexagon. The additional vertex in the figure corresponds to the edge we call $0(23)$.

with vertices 021, with 0 glued to 0, 1 to 2, and 2 to 1. And so on. Note the software Regina [1] and SnapPy [5] can be used to confirm that the manifold produced is the Whitehead link complement.

In the triangulation, tetrahedra 3 and 4 are the only ones meeting one of the cusps, in vertices $3(3)$ and $4(3)$, respectively. Moreover, we have chosen the labelling so that the Neumann–Zagier matrix satisfies the conditions of Lemma 3.4: see below. We will perform Dehn filling on the Whitehead link by removing these two tetrahedra and plugging in a layered solid torus.

The cusp neighbourhood of the resulting manifold is as shown in Figure 16, where the shaded hexagon shown there will be filled in by the cusp triangulation of the appropriate layered solid torus.

When we pull out tetrahedra 3 and 4, we are left with a manifold with punctured torus boundary. The slopes of these boundary curves can be computed in terms of the usual meridian/longitude of the cusp of the Whitehead link to be $3/1$, $2/1$, and $1/0 = \infty$ (we used Regina [1] and SnapPy [5] to compare slopes under Dehn filling to identify these edges). Each slope corresponds to an edge of the punctured torus, which corresponds to an edge of the triangulation, and appears twice in the hexagon of our cusp triangulation. The three slopes are labelled in Figure 16. There are two additional edges; one e only meets tetrahedra 3 and 4. The other we denote by $0(23)$ (because the edge $0(23)$ in Regina notation corresponds to this edge class).

We choose generators of the fundamental group of the cusp torus to be disjoint from the hexagon in the cusp neighbourhood. Then the entries of the incidence matrix for the Whitehead link are given as follows.

$$\begin{array}{c}
 E_{0(23)} \\
 E_{3/1} \\
 E_{2/1} \\
 E_{1/0} \\
 E_e \\
 m_0 \\
 l_0 \\
 m_1 \\
 l_1
 \end{array}
 \left[\begin{array}{c|c|c|c|c}
 \Delta_0 & \Delta_1 & \Delta_2 & \Delta_3 & \Delta_4 \\
 \hline
 \begin{array}{ccc} 1 & 0 & 0 \end{array} & \begin{array}{ccc} 0 & 0 & 1 \end{array} & \begin{array}{ccc} 0 & 0 & 2 \end{array} & \begin{array}{ccc} 0 & 0 & 0 \end{array} & \begin{array}{ccc} 0 & 0 & 0 \end{array} \\
 \hline
 \begin{array}{ccc} 0 & 1 & 0 \end{array} & \begin{array}{ccc} 1 & 0 & 0 \end{array} & \begin{array}{ccc} 0 & 1 & 0 \end{array} & \begin{array}{ccc} 1 & 0 & 0 \end{array} & \begin{array}{ccc} 1 & 0 & 0 \end{array} \\
 \begin{array}{ccc} 1 & 0 & 0 \end{array} & \begin{array}{ccc} 0 & 0 & 1 \end{array} & \begin{array}{ccc} 0 & 0 & 0 \end{array} & \begin{array}{ccc} 0 & 1 & 0 \end{array} & \begin{array}{ccc} 0 & 1 & 0 \end{array} \\
 \begin{array}{ccc} 0 & 1 & 2 \end{array} & \begin{array}{ccc} 1 & 2 & 0 \end{array} & \begin{array}{ccc} 2 & 1 & 0 \end{array} & \begin{array}{ccc} 0 & 0 & 1 \end{array} & \begin{array}{ccc} 0 & 0 & 1 \end{array} \\
 \hline
 \begin{array}{ccc} 0 & 0 & 0 \end{array} & \begin{array}{ccc} 0 & 0 & 0 \end{array} & \begin{array}{ccc} 0 & 0 & 0 \end{array} & \begin{array}{ccc} 1 & 1 & 1 \end{array} & \begin{array}{ccc} 1 & 1 & 1 \end{array} \\
 \hline
 \begin{array}{ccc} 0 & 0 & 1 \end{array} & \begin{array}{ccc} 0 & -1 & 0 \end{array} & \begin{array}{ccc} 0 & 0 & 0 \end{array} & \begin{array}{ccc} 0 & 0 & 0 \end{array} & \begin{array}{ccc} 0 & 0 & 0 \end{array} \\
 \begin{array}{ccc} 0 & -1 & 1 \end{array} & \begin{array}{ccc} 1 & -1 & 0 \end{array} & \begin{array}{ccc} 0 & 0 & 0 \end{array} & \begin{array}{ccc} 0 & 0 & 0 \end{array} & \begin{array}{ccc} 0 & 0 & 0 \end{array} \\
 \begin{array}{ccc} 0 & 0 & 0 \end{array} & \begin{array}{ccc} 0 & 0 & 0 \end{array} & \begin{array}{ccc} 0 & 0 & 0 \end{array} & \begin{array}{ccc} 1 & 0 & 0 \end{array} & \begin{array}{ccc} -1 & 0 & 0 \end{array} \\
 \begin{array}{ccc} 0 & 0 & 0 \end{array} & \begin{array}{ccc} 0 & 0 & 0 \end{array} & \begin{array}{ccc} 0 & 0 & 0 \end{array} & \begin{array}{ccc} 0 & 1 & 0 \end{array} & \begin{array}{ccc} 0 & -1 & 0 \end{array}
 \end{array} \right]$$

We now find the Neumann–Zagier matrix and sign vector C :

$$\text{NZ} = \begin{array}{c} E_{0(23)} \\ E_{3/1} \\ E_{2/1} \\ E_{1/0} \\ E_e \\ m_0 \\ l_0 \\ m_1 \\ l_1 \end{array} \left[\begin{array}{c|c|c|c|c}
 \Delta_0 & \Delta_1 & \Delta_2 & \Delta_3 & \Delta_4 \\
 \hline
 \begin{array}{cc} 1 & 0 \end{array} & \begin{array}{cc} -1 & -1 \end{array} & \begin{array}{cc} -2 & -2 \end{array} & \begin{array}{cc} 0 & 0 \end{array} & \begin{array}{cc} 0 & 0 \end{array} \\
 \hline
 \begin{array}{cc} 0 & 1 \end{array} & \begin{array}{cc} 1 & 0 \end{array} & \begin{array}{cc} 0 & 1 \end{array} & \begin{array}{cc} 1 & 0 \end{array} & \begin{array}{cc} 1 & 0 \end{array} \\
 \begin{array}{cc} 1 & 0 \end{array} & \begin{array}{cc} -1 & -1 \end{array} & \begin{array}{cc} 0 & 0 \end{array} & \begin{array}{cc} 0 & 1 \end{array} & \begin{array}{cc} 0 & 1 \end{array} \\
 \begin{array}{cc} -2 & -1 \end{array} & \begin{array}{cc} 1 & 2 \end{array} & \begin{array}{cc} 2 & 1 \end{array} & \begin{array}{cc} -1 & -1 \end{array} & \begin{array}{cc} -1 & -1 \end{array} \\
 \hline
 \begin{array}{cc} 0 & 0 \end{array} & \begin{array}{cc} 0 & 0 \end{array} & \begin{array}{cc} 0 & 0 \end{array} & \begin{array}{cc} 0 & 0 \end{array} & \begin{array}{cc} 0 & 0 \end{array} \\
 \hline
 \begin{array}{cc} -1 & -1 \end{array} & \begin{array}{cc} 0 & -1 \end{array} & \begin{array}{cc} 0 & 0 \end{array} & \begin{array}{cc} 0 & 0 \end{array} & \begin{array}{cc} 0 & 0 \end{array} \\
 \begin{array}{cc} -1 & -2 \end{array} & \begin{array}{cc} 1 & -1 \end{array} & \begin{array}{cc} 0 & 0 \end{array} & \begin{array}{cc} 0 & 0 \end{array} & \begin{array}{cc} 0 & 0 \end{array} \\
 \begin{array}{cc} 0 & 0 \end{array} & \begin{array}{cc} 0 & 0 \end{array} & \begin{array}{cc} 0 & 0 \end{array} & \begin{array}{cc} 1 & 0 \end{array} & \begin{array}{cc} -1 & 0 \end{array} \\
 \begin{array}{cc} 0 & 0 \end{array} & \begin{array}{cc} 0 & 0 \end{array} & \begin{array}{cc} 0 & 0 \end{array} & \begin{array}{cc} 0 & 1 \end{array} & \begin{array}{cc} 0 & -1 \end{array}
 \end{array} \right] \quad C = \begin{bmatrix} -1 \\ 2 \\ 1 \\ -2 \\ 0 \\ -1 \\ -1 \\ 0 \\ 0 \end{bmatrix}$$

Notice that the vector $B = [1, 1, 1, -1, 1, 0, 0, 0, 0, 0]^T$ satisfies the properties of Lemma 3.5: $\text{NZ} \cdot B = C$ and the last four entries of B are all zero.

We now wish to perform Dehn fillings. We will remove tetrahedra Δ_3 and Δ_4 , and attach an appropriate layered solid torus to obtain the desired Dehn filling. Figure 17 shows where we begin in the Farey graph, in the triangle T_0 with slopes $3/1, 2/1, 1/0$, and paths we can take to obtain well-known Dehn fillings, in particular twist knots.

For example, if we attach a degenerate layered solid torus, folding along the edge of slope $1/0$, we will perform $1/1$ Dehn filling, which gives the trefoil knot complement. To obtain other twist knots, first cover slope $1/0$, stepping into triangle T_1 in the Farey graph, then swing L into triangle T_2 . From there, the path taken depends on whether we wish to obtain an even twist knot or an odd one.

We now work through a few steps in the construction of Section 3, showing in detail how we obtain the Ptolemy equations for various twist knots.

The first step in the process is to remove Δ_3 and Δ_4 , obtaining a manifold M_0 with boundary consisting of two ideal triangles, and to construct the matrix NZ_0 from NZ . This matrix is given by stripping off rows corresponding to m_1 and l_1 and columns corresponding to Δ_3 and Δ_4 . Similarly, we obtain C_0 from C by removing two entries and adding 2 to one of the rows, as in Lemma 3.6. With our labelling, we add 2 to the row $E_{1/0}$.

$$\text{NZ}_0 = \begin{array}{c} E_{0(23)} \\ E_{3/1} \\ E_{2/1} \\ E_{1/0} \\ m_0 \\ l_0 \end{array} \left[\begin{array}{c|c|c}
 \Delta_0 & \Delta_1 & \Delta_2 \\
 \hline
 \begin{array}{cc} 1 & 0 \end{array} & \begin{array}{cc} -1 & -1 \end{array} & \begin{array}{cc} -2 & -2 \end{array} \\
 \hline
 \begin{array}{cc} 0 & 1 \end{array} & \begin{array}{cc} 1 & 0 \end{array} & \begin{array}{cc} 0 & 1 \end{array} \\
 \begin{array}{cc} 1 & 0 \end{array} & \begin{array}{cc} -1 & -1 \end{array} & \begin{array}{cc} 0 & 0 \end{array} \\
 \begin{array}{cc} -2 & -1 \end{array} & \begin{array}{cc} 1 & 2 \end{array} & \begin{array}{cc} 2 & 1 \end{array} \\
 \hline
 \begin{array}{cc} -1 & -1 \end{array} & \begin{array}{cc} 0 & -1 \end{array} & \begin{array}{cc} 0 & 0 \end{array} \\
 \begin{array}{cc} -1 & -2 \end{array} & \begin{array}{cc} 1 & -1 \end{array} & \begin{array}{cc} 0 & 0 \end{array}
 \end{array} \right] \quad C_0 = \begin{bmatrix} -1 \\ 2 \\ 1 \\ 0 \\ -1 \\ -1 \end{bmatrix}$$

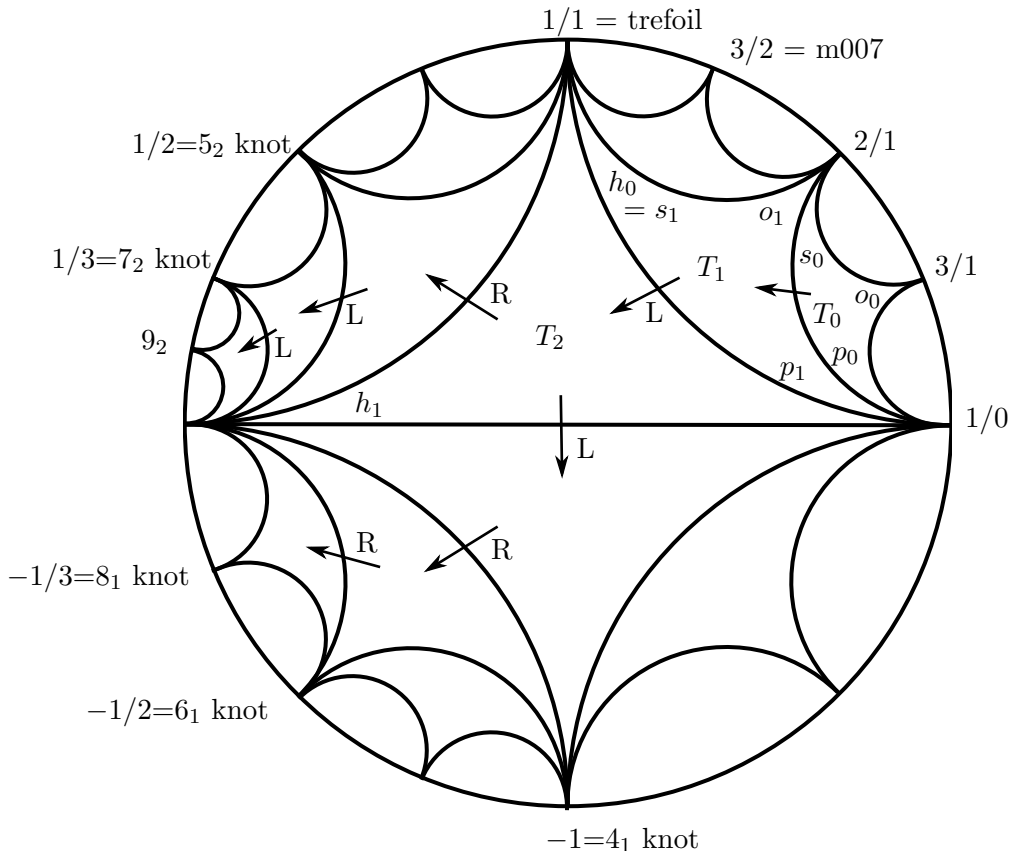


FIGURE 17. Some Dehn fillings of the Whitehead link and their location in the Farey graph.

Now use Lemma 3.13 to obtain a vector B_0 such that $C_0 - NZ_0 \cdot B_0$ consists of all zeros, except for a 2 in the entry corresponding to the edge with slope p_0 , which is the edge $E_{1/0}$.

$$B_0 = [1, 1, 1, -1, 1, 0]^T$$

To perform $1/1$ Dehn filling, to obtain the trefoil knot complement, at this step we would attach a degenerate layered solid torus. This is obtained by identifying two triangles on the boundary of M_0 by folding over the edge $3/1$, identifying edges $E_{2/1}$ and $E_{1/0}$. Thus, according to Lemma 3.9, the Neumann–Zagier matrix $NZ(1/1)$ of this triangulation of the trefoil complement is given as follows, along with sign vector $C(1/1)$:

$$NZ(1/1) = \begin{array}{c} E_{0(23)} \\ E_{3/1} \\ E_{2/1} + E_{1/0} \\ m_0 \\ l_0 \end{array} \left[\begin{array}{cc|cc|cc} & \Delta_0 & & \Delta_1 & & \Delta_2 \\ \hline 1 & 0 & -1 & -1 & -2 & -2 \\ 0 & 1 & 1 & 0 & 0 & 1 \\ -1 & -1 & 0 & 1 & 2 & 1 \\ -1 & -1 & 0 & -1 & 0 & 0 \\ -1 & -2 & 1 & -1 & 0 & 0 \end{array} \right] \quad C_0 = \begin{bmatrix} -1 \\ 2 \\ -1 \\ -1 \\ -1 \end{bmatrix}$$

Note that $NZ(1/1) \cdot B_0 = C(1/1)$, as predicted by Lemma 3.16.

We obtain the following Ptolemy equations from Definition 2.63:

$$\begin{aligned}
 \Delta_0 : & \quad (-1)^1 \ell^{-(1)/2} m^{(-1)/2} \gamma_{0(23)} \gamma_{2/1} + (-1)^1 \ell^{-(1)/2} m^{(-2)/2} \gamma_{3/1} \gamma_{1/0} - \gamma_{1/0}^2 = 0 \\
 & \quad \text{or} \quad -\ell^{1/2} m^{-1/2} \gamma_{0(23)} \gamma_{2/1} - \ell^{1/2} m^{-1} \gamma_{3/1} \gamma_{1/0} - \gamma_{1/0}^2 = 0 \\
 \Delta_1 : & \quad (-1)^{-1} \ell^{0/2} m^{1/2} \gamma_{3/1} \gamma_{1/0} + (-1)^1 \ell^{-(1)/2} m^{(-1)/2} \gamma_{1/0}^2 - \gamma_{0(23)} \gamma_{2/1} = 0 \\
 & \quad \text{or} \quad -m^{1/2} \gamma_{3/1} \gamma_{1/0} - \ell^{1/2} m^{-1/2} \gamma_{1/0}^2 - \gamma_{0(23)} \gamma_{2/1} = 0 \\
 \Delta_2 : & \quad \gamma_{1/0}^2 - \gamma_{1/0} \gamma_{3/1} - \gamma_{0(23)}^2 = 0
 \end{aligned}$$

(These are precisely equations 1.6–1.8 of Section 1.4.)

Finally, the Ptolemy equation for the trefoil are obtained by setting $\gamma_{2/1} = \gamma_{1/0}$. However, the trefoil is not hyperbolic, and our results do apply.

We next consider performing $-1/1$ Dehn filling, to obtain the complement of the 4_1 knot, also known as the figure-8 knot. This Dehn filling is obtained by attaching a layered solid torus built of two tetrahedra, $\Delta_{3/1}$ and $\Delta_{2/1}$, where our naming convention is as in Section 3.5: the tetrahedron at the k th step is labeled Δ_{o_k} .

Tetrahedron $\Delta_{o_0} = \Delta_{3/1}$ is attached when we step from T_0 to T_1 in the Farey graph. We obtain NZ_1 , C_1 , and B_1 :

$$\text{NZ}_1 = \begin{array}{c} E_{0(23)} \\ E_{3/1} \\ E_{2/1} \\ E_{p_0}=E_{1/0} \\ E_{h_0}=E_{1/1} \\ m_0 \\ t_0 \end{array} \left[\begin{array}{cc|cc|cc|cc} \Delta_0 & & \Delta_1 & & \Delta_2 & & \Delta_{3/1} & \\ \hline 1 & 0 & -1 & -1 & -2 & -2 & 0 & 0 \\ \hline 0 & 1 & 1 & 0 & 0 & 1 & 1 & 0 \\ \hline 1 & 0 & -1 & -1 & 0 & 0 & 0 & 2 \\ \hline -2 & -1 & 1 & 2 & 2 & 1 & -2 & -2 \\ \hline 0 & 0 & 0 & 0 & 0 & 0 & 1 & 0 \\ \hline -1 & -1 & 0 & -1 & 0 & 0 & 0 & 0 \\ \hline -1 & -2 & 1 & -1 & 0 & 0 & 0 & 0 \end{array} \right] C_1 = \begin{bmatrix} -1 \\ 2 \\ 1 \\ -2 \\ 2 \\ -1 \\ -1 \end{bmatrix}$$

Apply Lemma 3.14 to obtain B_1 such that $C_1 - \text{NZ}_1 \cdot B_1$ consists of all zeros, except for a 2 in the entry corresponding to the edge $E_{h_0} = E_{1/1}$.

$$B_1 = [1, 1, 1, -1, 1, 0, 0, 0]^T$$

Tetrahedron $\Delta_{o_1} = \Delta_{2/1}$ is attached when we step from T_1 to T_2 in the Farey graph; notice that the step in the Farey graph is in the direction L. Thus we obtain:

$$\text{NZ}_2 = \begin{array}{c} E_{0(23)} \\ E_{3/1} \\ E_{2/1} \\ E_{p_1}=E_{1/0} \\ E_{1/1} \\ E_{h_1}=E_{0/1} \\ m_0 \\ t_0 \end{array} \left[\begin{array}{cc|cc|cc|cc|cc} \Delta_0 & & \Delta_1 & & \Delta_2 & & \Delta_{3/1} & & \Delta_{2/1} & \\ \hline 1 & 0 & -1 & -1 & -2 & -2 & 0 & 0 & 0 & 0 \\ \hline 0 & 1 & 1 & 0 & 0 & 1 & 1 & 0 & 0 & 0 \\ \hline 1 & 0 & -1 & -1 & 0 & 0 & 0 & 2 & 1 & 0 \\ \hline -2 & -1 & 1 & 2 & 2 & 1 & -2 & -2 & -2 & -2 \\ \hline 0 & 0 & 0 & 0 & 0 & 0 & 1 & 0 & 0 & 2 \\ \hline 0 & 0 & 0 & 0 & 0 & 0 & 0 & 0 & 1 & 0 \\ \hline -1 & -1 & 0 & -1 & 0 & 0 & 0 & 0 & 0 & 0 \\ \hline -1 & -2 & 1 & -1 & 0 & 0 & 0 & 0 & 0 & 0 \end{array} \right] C_2 = \begin{bmatrix} -1 \\ 2 \\ 1 \\ -4 \\ 2 \\ 2 \\ -1 \\ -1 \end{bmatrix}$$

Now Lemma 3.15 gives B_2 . Note B_2 ends in $(0, 1)$ because we turned L in the Farey graph.

$$B_2 = [1, 1, 1, -1, 1, 0, 0, 0, 0, 1]^T$$

To obtain the 4_1 knot, from T_2 we fold over the edge $E_{1/1}$, identifying $E_{0/1}$ and $E_{1/0}$. Lemma 3.9 tells us how to obtain $\text{NZ}(-1/1)$ and $C(-1/1)$ from NZ_2 and C_2 . The vector B_2 will satisfy $\text{NZ}(-1/1) \cdot B_2 = C(-1/1)$ by Lemma 3.16. Then again we may read the Ptolemy equations off of $\text{NZ}(-1/1)$ and the sign vector B_2 . Notice that the first three Ptolemy equations, corresponding to Δ_0 , Δ_1 , and Δ_2 , are unchanged from above: this is because our matrices NZ_j do not change the

entries of NZ_0 , and similarly for adjustments to B_j . The new equations, arising from the layered solid torus, can actually be computed with reference only to Theorem 3.18, without writing down the full Neumann–Zagier matrix. We pick up two new equations as follows:

$$\begin{aligned}\Delta_{3/1} : \quad & \gamma_{3/1}\gamma_{1/1} + \gamma_{2/1}^2 - \gamma_{1/0}^2 = 0 \\ \Delta_{2/1} : \quad & -\gamma_{2/1}\gamma_{0/1} + \gamma_{1/1}^2 - \gamma_{1/0}^2 = 0\end{aligned}$$

(These are (1.9) and (1.10) of Section 1.4.) The equations for the figure-8 knot are finally obtained by setting the variables $\gamma_{0/1}$ and $\gamma_{1/0}$.

Now consider the 5_2 knot. This is obtained by starting with the same two tetrahedra $\Delta_{3/1}$ and $\Delta_{2/1}$ as in the case of the figure-8 knot. However, instead of folding across the edge $E_{1/1}$, we fold across the edge $E_{1/0}$, and identify $E_{1/1}$ to $E_{0/1}$; see Figure 17. Thus the Ptolemy equations look identical to those above for the figure-8 knot, except set the variables $\gamma_{1/1}$ and $\gamma_{0/1}$ to be equal.

For the 7_2 knot: turn right from the triangle T_2 in the Farey graph, picking up equation:

$$\Delta_{1/0} : \quad \gamma_{1/0}\gamma_{1/2} + \gamma_{1/1}^2 - \gamma_{0/1}^2 = 0,$$

((1.11) of Section 1.4) and identify variables $\gamma_{1/2}$ and $\gamma_{0/1}$.

For the 9_2 knot: Turn left. Pick up a new equation:

$$\Delta_{1/1} : \quad -\gamma_{1/1}\gamma_{1/3} + \gamma_{1/2}^2 - \gamma_{0/1}^2 = 0,$$

((1.12) of Section 1.4) and identify variables $\gamma_{1/3}$ and $\gamma_{0/1}$.

Any twist knot with $2N + 1$ crossings is obtained similarly, for $N \geq 4$. The word W in the Farey graph has the form LRL...L. The Ptolemy equations include all the equations above, as well as a sequence of equations

$$-\gamma_{1/k}\gamma_{1/(k+2)} + \gamma_{1/(k+1)}^2 - \gamma_{0/1}^2 = 0, \text{ for } 2 \leq k \leq N - 1.$$

At the end, the variables $\gamma_{0/1}$ and $\gamma_{1/N-1}$ are identified.

REFERENCES

- [1] Benjamin A. Burton, Ryan Budney, William Pettersson, et al., *Regina: Software for low-dimensional topology*, <http://regina-normal.github.io/>, 1999–2019. [24, 39, 40]
- [2] Abhijit Ashok Champanerkar, *A-polynomial and Bloch invariants of hyperbolic 3-manifolds*, ProQuest LLC, Ann Arbor, MI, 2003, Thesis (Ph.D.)—Columbia University. [1, 4, 10]
- [3] D. Cooper, M. Culler, H. Gillet, D. D. Long, and P. B. Shalen, *Plane curves associated to character varieties of 3-manifolds*, *Invent. Math.* **118** (1994), no. 1, 47–84. [1]
- [4] D. Cooper and D. D. Long, *Remarks on the A-polynomial of a knot*, *J. Knot Theory Ramifications* **5** (1996), no. 5, 609–628. [1]
- [5] Marc Culler, Nathan M. Dunfield, Matthias Goerner, and Jeffrey R. Weeks, *SnapPy, a computer program for studying the geometry and topology of 3-manifolds*, Available at <http://snappy.computop.org>, 2016. [40]
- [6] Tudor Dimofte, *Quantum Riemann surfaces in Chern-Simons theory*, *Adv. Theor. Math. Phys.* **17** (2013), no. 3, 479–599. [2, 4, 14, 16]
- [7] Tudor Dimofte and Roland van der Veen, *A Spectral Perspective on Neumann-Zagier*, arxiv:1403.5215, 2014. [2]
- [8] Vladimir Fock and Alexander Goncharov, *Moduli spaces of local systems and higher Teichmüller theory*, *Publ. Math. Inst. Hautes Études Sci.* (2006), no. 103, 1–211. [1, 5]
- [9] Sergey Fomin, Michael Shapiro, and Dylan Thurston, *Cluster algebras and triangulated surfaces. I. Cluster complexes*, *Acta Math.* **201** (2008), no. 1, 83–146. [5]
- [10] Sergey Fomin, Lauren Williams, and Andrei Zelevinsky, *Introduction to Cluster Algebras. Chapters 1–3*, arxiv:1608.05735, 2016. [5]
- [11] Stavros Garoufalidis, Dylan P. Thurston, and Christian K. Zickert, *The complex volume of $SL(n, \mathbb{C})$ -representations of 3-manifolds*, *Duke Math. J.* **164** (2015), no. 11, 2099–2160. [1, 2]
- [12] Michael Gekhtman, Michael Shapiro, and Alek Vainshtein, *Cluster algebras and Weil-Petersson forms*, *Duke Math. J.* **127** (2005), no. 2, 291–311. [5]
- [13] Matthias Goerner and Christian K. Zickert, *Triangulation independent Ptolemy varieties*, *Math. Z.* **289** (2018), no. 1-2, 663–693. [10]

- [14] François Guéritaud and Saul Schleimer, *Canonical triangulations of Dehn fillings*, *Geom. Topol.* **14** (2010), no. 1, 193–242. [5, 25]
- [15] Kazuhiro Hikami and Rei Inoue, *Braids, complex volume and cluster algebras*, *Algebr. Geom. Topol.* **15** (2015), no. 4, 2175–2194. [23]
- [16] Jim Hoste and Patrick D. Shanahan, *A formula for the A-polynomial of twist knots*, *J. Knot Theory Ramifications* **13** (2004), no. 2, 193–209. [6]
- [17] William Jaco and Hyam Rubinstein, *Layered triangulations of 3-manifolds*, arXiv:math/0603601, 2006. [5, 25]
- [18] William Jaco and J. Hyam Rubinstein, *0-efficient triangulations of 3-manifolds*, *J. Differential Geom.* **65** (2003), no. 1, 61–168. [23]
- [19] Daniel V. Mathews, *Erratum: An explicit formula for the A-polynomial of twist knots*, *J. Knot Theory Ramifications* **23** (2014), no. 11, 1492001, 1. [6]
- [20] ———, *An explicit formula for the A-polynomial of twist knots*, *J. Knot Theory Ramifications* **23** (2014), no. 9, 1450044, 5. [6]
- [21] Walter D. Neumann, *Combinatorics of triangulations and the Chern-Simons invariant for hyperbolic 3-manifolds*, *Topology '90* (Columbus, OH, 1990), Ohio State Univ. Math. Res. Inst. Publ., vol. 1, de Gruyter, Berlin, 1992, pp. 243–271. [2, 3, 19]
- [22] Walter D. Neumann and Don Zagier, *Volumes of hyperbolic three-manifolds*, *Topology* **24** (1985), no. 3, 307–332. [2, 6, 13, 14, 16]
- [23] Morris Newman, *Integral matrices*, Academic Press, New York-London, 1972, Pure and Applied Mathematics, Vol. 45. [4]
- [24] R. C. Penner, *The decorated Teichmüller space of punctured surfaces*, *Comm. Math. Phys.* **113** (1987), no. 2, 299–339. [5]
- [25] Henry Segerman, *A generalisation of the deformation variety*, *Algebr. Geom. Topol.* **12** (2012), no. 4, 2179–2244. [10]
- [26] William P. Thurston, *Three-dimensional geometry and topology. Vol. 1*, Princeton Mathematical Series, vol. 35, Princeton University Press, Princeton, NJ, 1997, Edited by Silvio Levy. [8, 16]
- [27] Jeff Weeks, *Computation of hyperbolic structures in knot theory*, *Handbook of knot theory*, Elsevier B. V., Amsterdam, 2005, pp. 461–480. [23, 24]
- [28] Lauren K. Williams, *Cluster algebras: an introduction*, *Bull. Amer. Math. Soc. (N.S.)* **51** (2014), no. 1, 1–26. [5]
- [29] Christian K. Zickert, *Ptolemy coordinates, Dehn invariant and the A-polynomial*, *Math. Z.* **283** (2016), no. 1–2, 515–537. [1, 2, 4]

DEPARTMENT OF MATHEMATICS, UNIVERSITY OF CALIFORNIA, DAVIS, CA 95616

Email address: jahowie@ucdavis.edu

SCHOOL OF MATHEMATICS, MONASH UNIVERSITY, VIC 3800, AUSTRALIA

Email address: Daniel.Mathews@monash.edu

SCHOOL OF MATHEMATICS, MONASH UNIVERSITY, VIC 3800, AUSTRALIA

Email address: jessica.purcell@monash.edu